NASA Technical Memorandum 87696

EXPERIMENTAL AND ANALYTICAL GENERIC SPACE STATION DYNAMIC MODELS

W. Keith Belvin

NASA Langley Research Center

Harold H. Edighoffer

Edighoffer, Inc.

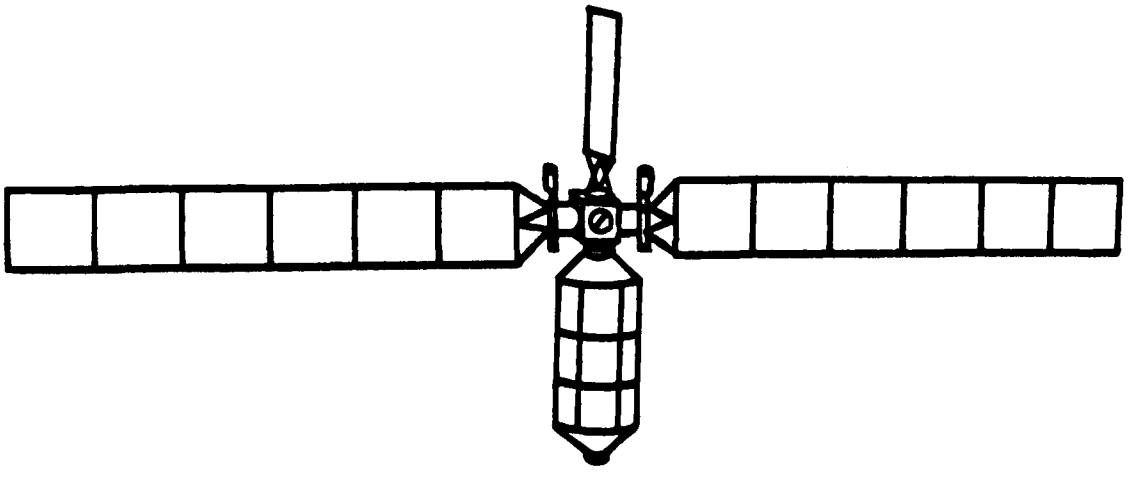

March 1986

National Aeronautics and Space Administration

Langley Research Center
Hampton, Virginia 23665

TABLE OF CONTENTS

INTRODUCTION

Verification of space station structural dynamic mathematical models will require special analysis and ground test methods. The size and flexibility of the space station conceptual configuration, Ref. 1, defies conventional testing of assembled flight hardware. Verification of the analysis must be performed through ground tests of scale models and full scale substructures. Even so, these ground test articles will be quite flexible. The interaction of this flexibility with the suspension system leads to uncertainties in the ground test results.

The vibration characteristics of a structure can be affected during ground testing by a number of factors such as suspension systems, gravity and ambient air. Suspension systems add stiffness to the structure and often result in coupling of low frequency structural modes and suspension system modes. Gravity loads can either increase or decrease the overall stiffness of a structure. Ambient air has both an apparent mass effect and a viscous damping effect. Scale model testing reduces the magnitude of these effects; however, joints and other key components of structures are difficult to scale due to minimum gage and tolerance restrictions.

The NASA Langley Research Center has a continuing program to improve ground test and analysis methods for extraction of the vibration characteristics of structures. As part of this program, a generic dynamic model has been designed and fabricated to assess the accuracy of analysis and test methods currently used in ground vibration testing. The configuration of the test model is a multi-body platform consisting of five substructures. The substructures are a semi-monocoque cylindrical habitation module, a square honeycomb sandwich radiator panel, two long slender honeycomb sandwich solar

arrays and a connecting cube. The interfaces among the four functional substructures and the connecting cube are identical allowing complete interchangeability for different configurations.

This report describes in detail the structure of the generic dynamic model and the analytical models used to predict the structural response. Considerations which affected the design are presented followed by a complete description of the model hardware. The finite element models used for prediction of test data are described in detail to permit replication of the analysis if desired.

DESIGN CONSIDERATIONS

Prior to the design of the space station reference configuration, Ref. 1, numerous space station concepts were being evaluated. Typical among these concepts was the Space Operation Center (SOC), Ref. 2. The SOC configuration consisted of cylindrical modules, solar array and radiator panels and interconnecting tunnels. The study herein used the elements of the SOC configuration to form a generic model as shown in Fig. 1. The model generality was maintained by designing each substructure with common interfaces. This scheme permitted the substructures to be rearranged to form different configurations. The substructures are attached with quick release marmon clamps. Marmon clamps allow each of the functional substructures to be rotated relative to the connecting cube and result in additional configuration flexibility.

The design of the substructure dimensions and stiffness was based on the expected use of the model. The intent was to simulate the general vibration characteristics of scaled space station models. Although no scale factor could be chosen in the absence of a full scale design, the frequencies of full scale components could be estimated by preliminary calculations as shown in Ref. 3. The estimated full scale fundamental flexible body frequencies are

Habitation Module	≈	10. Hz
Radiator	≈	1. Hz
Solar arrays	≈	0.1 Hz

To simulate a dynamically scaled model, the vibration frequencies of the model are increased inversely proportional to the scale factor. The substructures of the test model were designed with an approximate dynamic scale factor of

1/10. Thus, model substructure frequencies were chosen in the range of one order of magnitude greater than full scale.

The model habitation module is a relatively stiff substructure ($f_1 \approx 100$ Hz) and acts as a rigid body relative to the other substructures. Since preliminary calculations showed minimal changes in stiffness due to internal pressure, the habitation module was not pressurized during testing. The radiator panel is a structure of moderate stiffness ($f_1 \approx 10$ Hz) whereas the solar arrays are quite flexible ($f_1 \approx 1$ Hz). The solar arrays were constructed with six nearly square honeycomb sandwich panels that were bolted together at their tongue-and-groove interface joints. This construction allows flexibility to add or remove panels to change the frequency of the solar arrays as desired. The connecting cube used to attach the assemblage is very stiff ($f_1 = 300$ Hz) and can be treated as rigid.

A major design consideration was the ability to test the substructures separately and as an assemblage of substructures. The modular concept described above permits these tests provided a ground test suspension system can be designed to prevent overstressing of the structures due to their own weight. Two suspension systems were designed for the tests. First, a backstop fixture with a marmon clamp interface was designed to permit each substructure to be attached to a backstop for static and dynamic cantilever tests. The second suspension system consisted of cables attached to the substructures at strategic locations to simulate free-free boundary conditions. Although cable suspension cannot completely simulate free-free conditions, cable suspension was used during each substructure test and during the assemblage tests.

The final consideration of the design was the ability to slue the solar arrays. Sluing is a large angle transient maneuver that can produce substantial vibrations in flexible structures. For example, Ref. 4 describes the sluing response of flexible beam-like structures. The solar array support structures were hinged so the solar arrays could be rotated out-of-plane 180 degrees. All modal vibration tests were performed with the solar arrays locked at 90 degrees. However, vibration suppression tests have been performed using the root torque motor as an actuator.

EXPERIMENTAL MODEL

The assembled generic model is shown in Fig. 1 suspended in the NASA Langley Research Center 16-meter vacuum chamber. This is the vibration test configuration of the assembled structure. The structure schematic, shown in Fig. 2, indicates the principal dimensions and design features. The solar panel tip-to-tip width of the model is 348.60 inches and the overall length is 144.31 inches. All of the major components are made from 6061-T6 aluminum. This material was selected because of ease of fabrication, cost, and high strength-to-weight ratio. The 25.75 in. diameter by 68.61 in. long habitation module has a 0.032 in. thick skin and is a semi-monocoque ring stiffened cylinder with conical ends. The solar arrays are made of six nearly square aluminum honeycomb sandwich panels that are bolted together at the tongue-and-groove joint interfaces to make a total panel size of 150.47 in. by 25.24 in. The radiator is a single 46.75 in. square aluminum honeycomb sandwich panel oriented 90 degrees relative to the plane of the solar panels. The connecting cube consists of a framework of welded stiffeners with six interface rings all of the same size for interchangeability so that substructures can be attached to any of the six sides.

The following four sections describe the substructure hardware and fabrication in detail. Data contained in the analytical description of the model may be used to determine exact dimensions. Also, mass information for the experimental model may be obtained in the mass properties section.

Habitation Module

The habitation module concept was envisioned to have a diameter to length ratio similar to a full scale man rated habitation module. The full scale structure could be of sandwich construction and be designed to meet internal pressure and debris penetration requirements. Typical construction would involve internal rings to support storage and equipment racks and spherical ends to minimize stresses due to internal pressure. The test model was made of a single skin over stiffener rings and the ends were made conical to simplify fabrication.

The habitation module, shown in Fig. 3, is a three bay semi-monocoque ring stiffened cylinder with monocoque conical sections at each end. The conical sections are welded to marmon clamp rings for attachment to adjacent substructures. The entire construction is made from 6061-T6 aluminum. Figs. 4 and 5 show some of the subassembly details during fabrication.

The fabrication procedure required that six flat longitudinal strap-like longerons be used to hold the internal rings in place while the 0.032 in. thick curved skin sections were spot welded to the rings. The initial assembly step consisted of tack welding the two internal T-shaped rings and the two end rings, held in place by an assembly fixture, to strap longerons located at every 60 degrees. These strap longerons and internal T rings are shown in Fig. 4. The two rolled 0.032 in. thick skin sections, each covering 180 degrees, are then spot welded to the rings and the longitudinal straps. Two of the longitudinal straps are wider and act as internal splice plates. These wider splice plates have two rows of spot welds, one row for each skin section. The internal view of the completed cylindrical section is shown in Fig. 4.

The final assembly procedure was to attach the conical end section with 0.125 in. diameter cherry-max blind rivets to the cylindrical section. The 0.032 in. thick conical ends are made from spun aluminum sections welded to marmon clamp ring subassemblies. One of these completed conical end assemblies is shown in Fig. 5 being mated to the cylindrical section. Figure 6 shows the cherry-max blind rivet pattern.

Connecting Cube

The cube concept, with six interface connecting rings of the same size, was designed so that different substructures could be attached to any of the six locations by means of a marmon clamp. This quick release connection has the added capability of allowing attached substructures to be rotated relative to the connecting cube and clamped at any angle provided there is no physical interference with an adjacent substructure.

The connecting cube consists of a 12.80 in. cubic framework of internal angles along all of the edges welded together as shown in Fig. 6. The six connecting rings are welded to I beams that are also welded to the angle edge members. These internal I beams stiffen the connecting cube so they are capable of withstanding gravity induced bending loads. Figure 7 shows the completed connecting cube framework. The clamp ring interface-to-interface dimension is 16.40 in. At each of the I beam locations, an external triangular stiffener section was welded to the I beam and to the connecting rings as shown in Fig. 8. The final assembly step was to seam weld the 0.064 in. thick skins to the frame structure.

Marmon Clamp -- Figure 9 shows the relative size of the connecting cube, the habitation module and the marmon clamp. Figure 10 shows the completed cube attached to the habitation module with a marmon clamp. The marmon clamp used in this study is model MVT 89029-B-4-S-850-V. This clamp is a stainless steel V-retainer coupling with 8.5 inch nominal diameter and with an adjustable over center latch. A photograph of this clamp is shown in Fig. 11.

Radiator

The concept for the design of the experimental radiator was to make it square as opposed to the solar arrays that would be long rectangular appendages. Aluminum sandwich honeycomb construction was selected for light weight and the size was chosen such that the fabrication costs were not excessive. The size of the panel was made large enough so that the vibration frequencies would interact with the solar array frequencies and contribute to the lower frequencies of the model assemblage.

The radiator, shown in Fig. 12, is a single 46.75 in. square aluminum honeycomb sandwich panel. The 0.26 in. thick sandwich honeycomb has two 0.020 in. thick, 6061-T6 aluminum facings bonded to a 0.125 in. hexcell 5052 aluminum honeycomb core. The hexcell wall thickness is 0.001 in. This is the same configuration as that used in the solar arrays. The four edges have 6061-T6 beam elements that are bonded in place to encompass the honeycomb core. The base beam is a large T beam. The 5.00 in. dimension across the top of the T has sufficient area so that the tubular truss members can be welded to the outboard face. The center lip of the T is the same thickness as the core to act as an edge member and is cured in place using the same adhesive as

used to bond the facings to the core. The other three edge members are 6061-T6 rectangular beams having the same thickness as the core. The two skins are bonded to the four edge members and the hexcell core using the American Cyanamid FM 123-5 adhesive. The bonding is accomplished by using an autoclave. The hexcell core has breather holes and small holes were drilled in the facings to prevent internal pressure when testing in a vacuum. The panel is connected to the marmon clamp ring by a welded tube truss structure and a cylindrical aluminum ring subassembly. A marmon clamp ring is located at the interface end.

Solar Arrays

The solar arrays are the most flexible part of the space station. Numerous vibration modes dominated by solar array motion were anticipated at low frequencies. As such, the solar arrays were designed to be six nearly square aluminum honeycomb sandwich panels that are bolted together at tongue-and-groove interfaces. This construction provides the ability to add or remove panels to adjust the solar array natural frequencies as desired. The sandwich panels are 0.26 in. thick and are fabricated in the same manner as described in the radiator section. The completed six bay solar array assembly is shown in Fig. 13.

The solar array attachment assembly supports the six panels and is fastened to the connecting cube with a marmon clamp. The solar array attachment assembly is shown in Fig. 14. This assembly consists of a welded truss tubular support structure that is connected to the support cylinder through a shaft and double bearing hinge joint in series with an actuation motor that can rotate the solar array 180 degrees. The two bearing housings

and the actuating motor are fastened to an L shaped structure. This L shaped structure is bolted to the cap end of the cylindrical structure that mates to the connecting cube with a marmon clamp. The center section of the shaft is square, while the two ends that fit into the two bearings are circular. The other end of the truss structure is welded to the base edge member of the first sandwich panel.

Rotational Sluing -- Rotation of the solar arrays can be achieved by actuating the motor shown in Fig. 14. The motor is a TRW Globe Motor, Type BL No. 102A942-9. This motor is used for active sluing and vibration suppression of the solar arrays.

During the modal survey vibration tests, the motors and shaft were locked at 90 degrees by bolting two angles, at the solar array centerline, which rigidly connected the shaft to the L shaped framework. Figure 15 shows both the right and left solar arrays in the vibration test configuration. Figure 16 shows the solar array at the right rotated and the solar array at the left locked at the test position.

ANALYTICAL MODEL

The Engineering Analysis Language (EAL) finite element program, Ref. 5, was chosen to study and evaluate the generic model vibration modes and natural frequencies. Prestressed vibration analysis was performed to include gravity load effects. Six analytical models were developed, one for the assemblage of substructures and one for each substructure. The assemblage model is formed by rigidly connecting the substructure models at the appropriate interface nodes. Assemblage model interface nodes and substructure interface nodes have identical grid point numbers.

Figure 17 shows the undeformed shape of the analytical EAL space station model without the cable suspension system. Figure 18 shows the model divided into its five substructure models and also indicates the degree of grid refinement used. The assembled model has 621 grid points with 3726 degrees of freedom. There are 652 beam elements, 2 rod elements, 56 three-node plate elements, and 472 four-node plate elements. Rigid link offsets have been used to model beam members whose neutral axis was offset from the grid point locations. The origin of the global coordinate system for the assemblage model is located at the center of the connecting cube with the positive 1-axis in the direction of the right solar array and the positive 3-axis in the direction of the radiator as shown in Fig. 17.

The large number of degrees of freedom in the assemblage model required a special elimination sequence to be developed. The EAL processor SEQ, which automatically determines the joint elimination sequence, produced a decomposition sequence that required excessive computer storage during stiffness matrix decomposition. To circumvent this problem, a user-defined elimination sequence was developed using the technique given in Ref. 6. The user-defined

sequence was formed by first eliminating the grid points on the habitation module, starting at the end farthest from the connecting cube. Next, all of the grid points of the right solar array, starting at the end farthest from the connecting cube were eliminated. This procedure was repeated with the left solar array and then with the radiator and finally the remaining grid points of the connecting cube were eliminated.

The substructure analytical models will be described in two steps. First the grid point locations are defined for each model by a figure showing the important grid points to establish visual orientation. The complete tabulation of all of the grid point locations can be found in Tables 1-5. Secondly, the plate, beam, and rod elements that connect these grid points will be defined for each substructure. The EAL section properties (NSECT) of the beam elements are shown in Fig. 19. The text will refer to a particular NSECT when describing the beam elements. The assemblage model will be described implicitly during the discussion of the five substructure models. If there is an element in substructure A and another element in substructure B at a common interface, the assemblage model has both the A and B elements at this interface.

Habitation Module Analytical Model

The first substructure model discussed is the three bay habitation module. The station location of the plate elements and rings are shown in Fig. 20. The overall length is 68.61 in. and the maximum cylinder diameter is 25.57 in. The two end diameters are 6.50 inches. The station locations are measured in the negative 3-direction from the origin which is located at the center of the connecting cube. The habitation module grid points are shown in Fig. 21.

There are eight rings modeled as 16 straight beam elements at each of the eight stations shown in Fig. 20. All these rings except the two end rings are internal to the 0.032 in. thick skin. In Fig. 21, the two end rectangular rings, NSECT 18 in Fig. 19, at station -8.20 and -76.81 represent the lip of the marmon clamp and the stiffness of one half the marmon clamp. The first ring element connects the grid point at location A to the grid point at location B. The sixteenth ring element connects the grid point at location P to the grid point at location A to complete the sixteen element ring. The two rectangular rings at the intersection of the smaller end cylindrical section and the conical section, NSECT 17, at station -10.00 and -75.01, represent the tapered part of the machined end ring that mates with the conical section. The two angle rings, NSECT 16, at the intersection of the conical sections and the center cylindrical section, at station -18.89 and -66.12, represent the tapered-flange angle of the internal splice ring. The two center internal tee rings, NSECT 2, at station -34.63 and -50.38, in the cylindrical section represent the stabilizing rings.

The plate elements and their grid point numbers are shown in Fig. 22. The 0.032 in. thick rectangular plate elements cover the center cylindrical portion and 0.032 in. thick trapezoidal plate elements cover the two conical sections. The 0.100 in. thick plate elements at each end represents the wall thickness of the cylindrical portion of the machined end ring that has the marmon clamp lip at one end and a conical ring cross-section at the other end. The first sixteen 0.100 in. thick plate elements in Fig. 22 connect the grid points at station -76.81 with those at station -75.01. The first plate element connects grid points 33 and 34 at station -76.81 and grid points 49 and 50 at station -75.01. The sixteenth plate element connects grid point 48 and

33 at station -76.81 and grid points 64 and 49 at station -75.01. This sixteenth plate element completes the 360 degree arc of plate elements at this station location. The next 80 plate elements that are 0.032 in. thick connect the grid points shown in a similar manner resulting in five rows of plate elements with each row having sixteen plates in a 360 degree arc. Finally the last sixteen 0.100 in. thick plate elements connect the grid points at station -10.00 and -8.20 as shown.

Connecting Cube Analytical Model

The second EAL substructure model to be discussed is the connecting cube shown in Fig. 23. The origin of the global coordinate system is at the geometric center of the connecting cube. The grid points on each facing of the cube are located 6.40 in. from the origin and represent the center line of the 0.064 in. thick skin. Each cylinder extends 1.80 in. from the cube facing so that the attachment interfaces are 8.20 in. from the origin. The model has six attachment cylinders that have their grid points located on a 6.50 in. diameter. In Fig. 23, the aft, top and left faces are shown. Some of the grid points are shown to help in the orientation of Figs. 24 through 27. In these figures, the view is such that the viewer is looking inboard toward the origin. The numbers in parenthesis represent the global coordinate direction shown in Fig. 23.

There are six clamp rings located 8.20 in. from the origin on each of the six faces as shown in Fig. 24. There are 16, NSECT 18, rectangular beam elements located at each interface location, or a total of 96 elements. At the intersection of the facing and the attachment cylinder there is a second ring of rectangular beam elements, NSECT 19, that represents the ring flange of the

machined connecting cylinder subassembly. The cylindrical portion of this subassembly is represented in the model by sixteen 0.100 in. thick plate elements shown in Fig. 27.

The orientation of the connecting grid point locations for each of the six faces is determined by the coordinate directions AA and BB shown in the figure and the numbers in parenthesis following the label of the face. The first clamp ring beam element on the aft face connects grid point 382 to 383 from location A to location B with the global coordinate system such that AA is equal to 1 and is pointing right and BB is equal to 2 and pointing up. By referring back to Fig. 23, this orientation is established. The same procedure is used for the other faces and subsequent figures.

Along each of the twelve edges there are angle beam elements, NSECT 7, used to support the 0.064 in. thick skin as shown in Fig. 25. Because these beams are common to two faces, 96 beam elements are shown, each appearing twice in the figure. Also in Fig. 25, the 24 I-beam bending stiffeners are shown. Four of these bending stiffeners connect the ring on each of the six faces to the edge beams. This arrangement stiffens the entire connecting cube so that it can withstand the gravity induced bending loads when the substructures are attached to the connecting cube.

There are 96 plate elements, sixteen on each face, connecting the ring beam members to the edge beam members as shown in Fig. 26. Figure 27 shows the location of the 96 attachment cylinder plate elements, sixteen on each side of the connecting cube. On the aft face (see Fig. 23) the first row 382, 383, etc. is at the clamp ring 8.20 in. from the origin while the second row 398, 399, etc. is at the ring 6.40 in. from the origin. Figure 28 shows the location of the 24 triangular stiffeners.

Radiator Analytical Model

The third EAL substructure model to be discussed is the radiator model shown in Fig. 29. As previously stated, the origin of the global coordinate system is at the center of the connecting cube, not shown. The interface, at station 8.20, has the same 6.40 in. diameter as the connecting cube and has the same grid points. The 2.15 in. long truss support cylinder is represented by sixteen plate elements between station 8.20 and 10.35. From station 10.35 to 20.75, the tubular truss structure is modeled with six beam elements. The aluminum sandwich honeycomb radiator is 46.75 in. square and subdivided into 64 five layer plate elements as shown in Fig. 29. There are beam elements around the four edges to represent the stiffness of the aluminum honeycomb edge stiffeners. The base beam along station 20.75 is a stiff T-shaped beam to which the tubular truss rings are welded and to which the sandwich honeycomb panel is attached. This beam is modeled using eight beam elements. Around the other three sides, the smaller sandwich aluminum edge members are all the same and are represented by 24 beam elements in the finite element model.

The 64 radiator sandwich honeycomb plate elements and there connecting grid point numbers are shown in Fig. 30. The grid point locations are mapped by row and column so that all of the 64 plate elements are identified. The five layer laminate plate elements have the dimensions shown in the figure. These layers consist of the two 0.020 in. thick facings, the two 0.007 in. thick adhesive layers and the center honeycomb core. The total thickness is 0.260 in. Young's Modulus for the 6061-T6 aluminum facing was 10.0E+6 psi and for the 0.007 in. adhesive layers the value of 3.0E+6 psi was used. The 5052 aluminum honeycomb core had a 0.125 in. hex cell size and a 0.001 in. wall

thickness and contributed little to the total bending stiffness. Therefore, the extensional stiffness and bending stiffness of the core was set equal to zero and with the above properties, the effective adhesive thickness of 0.007 in. was calculated from static bending test data.

The radiator sandwich edge and base beam configurations, beam location and beam connecting grid point locations are shown in Fig. 31. The eight T-shaped base beam elements, NSECT 24, are 2.00 in. wide. The 24 rectangular edge beam elements, NSECT 23, extend around the other three sides connecting the grid points shown in the figure.

The radiator truss and ring beam elements and their connecting grid point locations are shown in Fig. 32. There are 6 tubular truss beam elements, NSECT 14, connecting the ring at station 10.35 with the base beam at station 20.75. There are 16 rectangular beam elements, NSECT 22, representing the truss ring at station 8.20 and 16 rectangular beam elements, NSECT 18, representing the interface ring at station 10.35. The radiator attachment cylinder plate elements and their connecting grid point numbers are also shown in Fig. 32. The 16 plate elements are 0.30 in. thick to represent the cylinder wall. The grid points are located at the center line of this wall thickness where the radius is 3.20 in.

Right Solar Array Analytical Model

The fourth EAL substructure model is the right solar array model shown in Fig. 33. The connecting cube-right solar array interface is 8.20 in. in the positive 1-coordinate direction from the center of the connecting cube. The solar array interface, as seen in Fig. 14, consists of a connecting cylinder with a bulkhead at the end closest to the solar array panels. A 5.00 in. by

0.50 in. L-shaped bearing and motor support beam is fastened to this bulkhead. A shaft, connected to the motor and supported by two bearings, is attached to the solar array panel assembly through a tubular truss structure. The size of the six bay panel assembly is 150.47 in. by 25.24 in.

The connecting cylinder has a 3.625 in. radius compared with the 3.25 in. radius of the connecting cube. To account for this difference in radius, the solar array connecting ring grid points were located at a radius of 3.25 in. and the cylinder plate element grid points were connected to a second row of grid points at a radius of 3.625 in. The interface ring grid points are common for the connecting cube and the right solar array. The ring grid points and the cylinder plate grid points were connected by stiff radial beam elements.

The six bay aluminum sandwich honeycomb panels were subdivided into 24 plate elements, four in each bay, as shown in Fig. 34. There are beam elements along the four edges and cross beam elements at every second plate joint to represent the stiffness of the tongue and grove bolted joint that is used to attach the six bays together. The plate elements and their connecting grid point numbers are shown in Fig. 34. A five layer laminate plate element was used as indicated in the figure. These layers consist of the two 0.020 in. thick facings, the two 0.007 in. thick adhesive layers and the center honeycomb core. The total thickness is 0.260 in. This is the same sandwich honeycomb configuration used in the the radiator model. The grid point locations are mapped by row and column so that all 24 plate elements are identified.

The location and grid point connectivity of the right solar array edge and cross beam configurations are shown in Fig. 35. The two T-shaped base beam elements, NSECT 24, are stiff 2.00 in.-wide beams so that the distributed

panel loads can be transferred to the tubular truss. The 24 rectangular edge beam elements, NSECT 20, extend along the two sides connecting the grid points shown in the figure. The ten (10) rectangular cross beams, NSECT 21, represents the tongue beam of one of the adjacent bays combined with the groove beam of the other adjacent bay. The two end cross beams, NSECT 10, represent the T-shaped tongue beam at the end of the last bay.

The right solar array truss, shaft and L support beam elements and their connecting grid point locations are shown in Fig. 36. There are four tubular truss beam elements, NSECT 14, connecting the shaft at 15.08 in. with the base beam at 23.83 in. There are five square shaft beam elements, NSECT 13, located at 15.08 in. The actual shaft is square in the center with a circular cross section machined at each end where the bearings and motor attachments are located. There are six rectangular beam elements representing the L support beam. This beam has a depth of 5.00 in. and a width of 0.50 in. and has an arm to support the motor at grid point 548 making it L shaped. The two bearing beam elements had the same cross section as the support beam. The rotation of the shaft was modeled by defining two grid points at the same bearing location connected by a zero length beam element. The zero length beam element stiffness properties are represented by a stiffness matrix K. All of the off-diagonal terms of K are set equal to zero, whereas, the diagonal terms of K are set to zero for a pinned connection or to 1.0E+9 lb/in for a rigid connection.

The first bearing has common grid point numbers 546 and 547 and the second bearing has common grid points 544 and 545. The three extensional and two of the rotational degrees of freedom have a diagonal stiffness value of 1.0E+9 lb/in while the value of zero was used in the direction where free rotation was allowed. The model was also constructed so that a torsional spring could

be inserted at the motor-shaft interface connecting grid points 548 and 549. Again, these are common grid point locations connected by a zero length beam.

There are 2 rectangular attachment stiffener beams, NSECT 12, that connect the center line of the L support beam at grid point 539 to the bolt locations at grid point 538 and 540. These beams were added to introduce the proper loads into the bulkhead shown in Fig. 37 at grid point 538 and 540 where the bulkhead is bolted to the L support beam. The 0.50 in. thickness is the thickness of the L support beam and the 1.75 in. width is set equal to the length of the beam. The two clamp stiffener beams, NSECT 6, represent two clamp angles which were used to lock the solar arrays at 90 degrees. These beams connected the bulkhead bolts at grid point 538 and 540 to the shaft grid point 3 to restrict relative rotation between the shaft and the bulkhead. The cable attachment and loop beam are described in the Cable Suspension System section.

The right solar array support bulkhead and support cylinder plate elements and their connecting grid points are shown in Fig. 37. There are four four-node plate elements and sixteen three-node plate elements in the bulkhead that are 0.440 in. thick. The support cylinder plate element connecting grid points are mapped in Fig. 37 so the first row of grid point numbers represent the connection to the bulkhead located 12.42 in. from the origin in the 1 direction. This row is designated $A_o, B_o \ldots . P_o$ in the figure. The second row of grid point numbers are located at the interface plane located 8.20 in. from the origin. This row is designated $A_i, B_i \ldots . . P_i$ in the figure. All grid points are located at a radius of 3.625 in.

The interface ring beams, located 8.20 in. from the origin, and their connecting grid points are shown in Fig. 38. There are 16 circumferential beam elements, NSECT 18, representing the interface ring and half of the

marmon clamp. These beam elements connect the inner row of grid points that are common with the connecting cube interface grid points. There are 16 radial beam elements, NSECT 15, that connect the ring beam elements at a radius of 3.25 in. to the cylinder plate elements located at a radius of 3.625 in.

Left Solar Array Analytical Model

The fifth EAL substructure model is the left solar array model shown in Fig. 39. This substructure is nearly identical to the right solar array model shown in Fig. 33. If the right solar array is rotated 180 degrees around the global 2 axis, the left model is the same as the right model except the location of the motor and the cable attachment points are pointing in the wrong direction along the 3 axis. The grid point locations for the right solar array were generated using the right solar array coordinate system in Table 2 while the grid point locations for the left solar array used the left solar array coordinate system shown in Table 3. The right solar array coordinate system is rotated 90 degrees about the global 2 axis while the left solar array coordinate system is rotated -90 degrees about the global 2 axis. Table 6 shows the comparison of grid point numbers of the left and right solar arrays.

To determine the connecting grid point numbers for the left solar array sandwich honeycomb plate elements, increase the grid point numbers shown in Fig. 34 for the right side by the difference found in Table 6. The same is true for Figs. 35,37 and 38. Fig. 36 is replaced with Fig. 40 for the left solar array because the connectivity of the support beam.

CABLE SUSPENSION SYSTEM

To support the test models in a gravity environment, a cable suspension system was used. Free-free boundary conditions were desired; however, cable suspension systems produce pendulum modes that can couple with flexible model modes. Preliminary analysis indicated that the first flexible structural frequency of the generic model would be below 1 Hz. Since the amount of dynamic coupling between suspension modes and structure modes is strongly influenced by the frequency separation, Refs. 7 and 8, it was felt that the suspension system would affect the free-free structure vibration characteristics. Therefore, the suspension system was included in the analytical models. The philosophy was to test and correlate with analysis all the modes including the suspension modes and then determine the free-free modes of the structure using the verified analytical models.

In the test program, two cables were attached to the vacuum test chamber ceiling and the other end was attached to the model. Dimensions of the suspension system are shown in Fig. 41. Each cable was offset 49.25 in. from the point where the 3 axis intercepts the ceiling and had a total length of 572. in. The cables were nominally 0.125 in. diameter steel with helically wrapped 3X7 strand construction. The cable density was measured to be 0.002447 lb/in. The same cables were used for the assemblage tests as for each of the substructure tests.

In the analytical models, the cables were modeled as rod elements from the fixed attachment points at grid points 652 and 653 to the cable to model attachment points. The cable to model attachment grid points for the substructure tests are as follows:

Connecting Cube	214 and 267

Habitation Module	33 and 145
Radiator Panel	371 and 379
Right Solar Array Panel	191 and 203
Left Solar Array Panel	252 and 264

In the assemblage analysis model the cable to model attachment was formed by looping the cable around the solar array L support beams, as shown in Figs. 41 and 42. The cable loop triangle extends from grid point 1 to grid point 543 on the right L support beam, shown in Fig. 36, and from grid point 2 to grid point 537 on the left L support beam, shown in Fig. 40. It was determined the loop triangle produced rotational stiffness in the plane of the triangle. Thus, the two cables of the loop were modeled as a single beam element where the in-plane bending stiffness was set equal to the effective stiffness of the cable loop triangle.

MASS PROPERTIES

The masses of the analytical models were based on weight measurements of selected parts and on area calculations from fabrication drawings. Each complete substructure also was weighed and this weight was compared with the analytical model weights. The measured and analytical model weight comparison is given in Table 7. The total weight of all substructures was measured to be 194.9 lbs and the analysis model predicts 196.45 lbs.

The assemblage model center of gravity is located only 0.334 inches from the origin, close to the center of the connecting cube. The mass moments of inertia in mass units, lb-sec^2-in, and center of gravity locations in the global coordinate system for all six models are given in Table 8.

SUMMARY REMARKS

A generic dynamic model has been designed and fabricated to study ground vibration test and analysis methods. Finite element models have been developed to predict the structural response. Detailed descriptions of the test and analytical models are presented as reference information.

The dynamic test model consists of five substructures which can be interconnected in many configurations. Special features of the test model include quick release marmon clamps to fasten substructures together, torque motors to allow solar array sluing and vibration frequencies of less than one Hertz. Cable suspension systems were used in the ground vibration tests to simulate free-free boundary conditions.

The finite element models were developed using the Engineering Analysis Language (EAL) program. Six analytical models were developed, one of each substructure and one of the assemblage. Special features of the analytical models are modeling of the effective honeycomb adhesive thickness, inclusion of the cable suspension system and modeling of distributed gravity loads.

The information in this paper is intended for reference purposes. Results of the modal vibration tests and analysis described herein are documented in Ref. 9.

REFERENCES

1. Housner, J. M., "Structural Dynamics Model and Response of the Deployable Reference Configuration Space Station," NASA TM-86386, May, 1985.

2. Covington, C. and Piland, R. O., "Space Operations Center - Next goal for manned space flight.," Astronautics and Aeronautics, Vol. 18, Sept., 1980, pp 30-37.

3. Livingston, L. E., "Space Operations Center: A Concept Analysis," NASA TM-81062, Nov., 1979.

4. Juang, J. N. and Horta, L. G., "A Slewing Control Experiment for Flexible Structures," Proceedings of the Fifth VPI&SU/AIAA Symposium on Dynamics and Control of Large Structures, Blacksburg, Virginia, June 12-14, 1985, pp. 547-570.

5. Whetstone, W. D., "EISI-EAL Engineering Analysis Language Reference Manual," EISI-EAL System Level 2091, Vols. 1 and 2, Engineering Information Systems, Inc., San Jose, California, July, 1983.

6. Whetstone, W. D., "Computer Analysis of Large Space Frames," Journal of the Structural Division, ASCE, Vol. 95, No. ST 11, Nov., 1969, pp. 2401-2417.

7. Herr, R. W.: "Some Cable Suspension Systems and Their Effects on the Flexural Frequencies of Slender Aerospace Structures," NASA TN D-7693, Sept. 1974.

8. Hanks, B. R. and Pinson, L. D.: "Large Space Structures Raise Testing Challenges," Astronautics and Aeronautics, Oct. 1983, pp. 34-40.

9. Belvin, W. K. and Edighoffer, H. E.: "Dynamic Analysis and Experiment Methods for a Generic Space Station Model," AIAA/ASME/ASCE/AHS 27th Structures, Structural Dynamics and Materials Conference, AIAA paper no. 86-0838-CP, San Antonio, Texas , May 19-21, 1986.

TABLE 1. JOINT LOCATIONS IN GLOBAL COORDINATE SYSTEM

Joint No.	Global 1 (in.)	Global 2 (in.)	Global 3 (in.)
1	12.89	0.0	24.35
2	-12.89	0.0	24.35

Joint No.	Radial (in.)	Circumferential (deg.)	Global 3 (in.)
33	3.25	0.0	-76.812
34	3.25	22.5	-76.812
35	3.25	45.0	-76.812
36	3.25	67.5	-76.812
37	3.25	90.0	-76.812
38	3.25	112.5	-76.812
39	3.25	135.0	-76.812
40	3.25	157.5	-76.812
41	3.25	180.0	-76.812
42	3.25	202.5	-76.812
43	3.25	225.0	-76.812
44	3.25	247.5	-76.812
45	3.25	270.0	-76.812
46	3.25	292.5	-76.812
47	3.25	315.0	-76.812
48	3.25	337.5	-76.812
49	3.25	0.0	-75.012
50	3.25	22.5	-75.012
51	3.25	45.0	-75.012
52	3.25	67.5	-75.012
53	3.25	90.0	-75.012
54	3.25	112.5	-75.012
55	3.25	135.0	-75.012
56	3.25	157.5	-75.012
57	3.25	180.0	-75.012
58	3.25	202.5	-75.012
59	3.25	225.0	-75.012
60	3.25	247.5	-75.012
61	3.25	270.0	-75.012
62	3.25	292.5	-75.012
63	3.25	315.0	-75.012
64	3.25	337.5	-75.012
65	12.786	0.0	-66.122
66	12.786	22.5	-66.122
67	12.786	45.0	-66.122
68	12.786	67.5	-66.122
69	12.786	90.0	-66.122
70	12.786	112.5	-66.122
71	12.786	135.0	-66.122
72	12.786	157.5	-66.122
73	12.786	180.0	-66.122
74	12.786	202.5	-66.122
75	12.786	225.0	-66.122

Joint No.	Radial (in.)	Circumferential (deg.)	Global 3 (in.)
76	12.786	247.5	-66.122
77	12.786	270.0	-66.122
78	12.786	292.5	-66.122
79	12.786	315.0	-66.122
80	12.786	337.5	-66.122
81	12.786	0.0	-50.378
82	12.786	22.5	-50.378
83	12.786	45.0	-50.378
84	12.786	67.5	-50.378
85	12.786	90.0	-50.378
86	12.786	112.5	-50.378
87	12.786	135.0	-50.378
88	12.786	157.5	-50.378
89	12.786	180.0	-50.378
90	12.786	202.5	-50.378
91	12.786	225.0	-50.378
92	12.786	247.5	-50.378
93	12.786	270.0	-50.378
94	12.786	292.5	-50.378
95	12.786	315.0	-50.378
96	12.786	337.5	-50.378
97	12.786	0.0	-34.634
98	12.786	22.5	-34.634
99	12.786	45.0	-34.634
100	12.786	67.5	-34.634
101	12.786	90.0	-34.634
102	12.786	112.5	-34.634
103	12.786	135.0	-34.634
104	12.786	157.5	-34.634
105	12.786	180.0	-34.634
106	12.786	202.5	-34.634
107	12.786	225.0	-34.634
108	12.786	247.5	-34.634
109	12.786	270.0	-34.634
110	12.786	292.5	-34.634
111	12.786	315.0	-34.634
112	12.786	337.5	-34.634
113	12.786	0.0	-18.890
114	12.786	22.5	-18.890
115	12.786	45.0	-18.890
116	12.786	67.5	-18.890
117	12.786	90.0	-18.890
118	12.786	112.5	-18.890
119	12.786	135.0	-18.890
120	12.786	157.5	-18.890
121	12.786	180.0	-18.890
122	12.786	202.5	-18.890
123	12.786	225.0	-18.890
124	12.786	247.5	-18.890
125	12.786	270.0	-18.890

Joint No.	Radial (in.)	Circumferential (deg.)	Global 3 (in.)
126	12.786	292.5	-18.890
127	12.786	315.0	-18.890
128	12.786	337.5	-18.890
129	3.250	0.0	-10.000
130	3.250	22.5	-10.000
131	3.250	45.0	-10.000
132	3.250	67.5	-10.000
133	3.250	90.0	-10.000
134	3.250	112.5	-10.000
135	3.250	135.0	-10.000
136	3.250	157.5	-10.000
137	3.250	180.0	-10.000
138	3.250	202.5	-10.000
139	3.250	225.0	-10.000
140	3.250	247.5	-10.000
141	3.250	270.0	-10.000
142	3.250	292.5	-10.000
143	3.250	315.0	-10.000
144	3.250	337.5	-10.000
145	3.250	0.0	-8.200
146	3.250	22.5	-8.200
147	3.250	45.0	-8.200
148	3.250	67.5	-8.200
149	3.250	90.0	-8.200
150	3.250	112.5	-8.200
151	3.250	135.0	-8.200
152	3.250	157.5	-8.200
153	3.250	180.0	-8.200
154	3.250	202.5	-8.200
155	3.250	225.0	-8.200
156	3.250	247.5	-8.200
157	3.250	270.0	-8.200
158	3.250	292.5	-8.200
159	3.250	315.0	-8.200
160	3.250	337.5	-8.200
161	3.250	0.0	-6.400
162	3.250	22.5	-6.400
163	3.250	45.0	-6.400
164	3.250	67.5	-6.400
165	3.250	90.0	-6.400
166	3.250	112.5	-6.400
167	3.250	135.0	-6.400
168	3.250	157.5	-6.400
169	3.250	180.0	-6.400
170	3.250	202.5	-6.400
171	3.250	225.0	-6.400
172	3.250	247.5	-6.400
173	3.250	270.0	-6.400
174	3.250	292.5	-6.400
175	3.250	315.0	-6.400
176	3.250	337.5	-6.400

Joint No.	Global 1 (in.)	Globel 2 (in.)	Globel 3 (in.)
299	0.0	-23.375	67.50
300	0.0	-17.5313	67.50
301	0.0	-11.6875	67.50
302	0.0	-5.84375	67.50
303	0.0	0.0	67.50
304	0.0	5.84375	67.50
305	0.0	11.6875	67.50
306	0.0	17.5313	67.50
307	0.0	23.375	67.50
308	0.0	-23.375	61.6563
309	0.0	-17.5313	61.6563
310	0.0	-11.6875	61.6563
311	0.0	-5.84375	61.6563
312	0.0	0.0	61.6563
313	0.0	5.84375	61.6563
314	0.0	11.6875	61.6563
315	0.0	17.5313	61.6563
316	0.0	23.375	61.6563
317	0.0	-23.375	55.8125
318	0.0	-17.5313	55.8125
319	0.0	-11.6875	55.8125
320	0.0	-5.84375	55.8125
321	0.0	0.0	55.8125
322	0.0	5.84375	55.8125
323	0.0	11.6875	55.8125
324	0.0	17.5313	55.8125
325	0.0	23.375	55.8125
326	0.0	-23.375	49.9688
327	0.0	-17.5313	49.9688
328	0.0	-11.6875	49.9688
329	0.0	-5.84375	49.9688
330	0.0	0.0	49.9688
331	0.0	5.84375	49.9688
332	0.0	11.6875	49.9688
333	0.0	17.5313	49.9688
334	0.0	23.375	49.9688
335	0.0	-23.375	44.1250
336	0.0	-17.5313	44.1250
337	0.0	-11.6875	44.1250
338	0.0	-5.84375	44.1250
339	0.0	0.0	44.1250
340	0.0	5.84375	44.1250
341	0.0	11.6875	44.1250
342	0.0	17.5313	44.1250
343	0.0	23.375	44.1250
344	0.0	-23.375	38.2813
345	0.0	-17.5313	38.2813
346	0.0	-11.6875	38.2813
347	0.0	-5.84375	38.2813
348	0.0	0.0	38.2813
349	0.0	5.84375	38.2813

Joint No.	Global 1 (in.)	Global 2 (in.)	Global 3 (in.)
350	0.0	11.6875	38.2813
351	0.0	17.5313	38,2813
352	0.0	23.375	38.2813
353	0.0	-23.375	32.4375
354	0.0	-17.5313	32.4375
355	0.0	-11.6875	32.4375
356	0.0	-5.84375	32.4375
357	0.0	0.0	32.4375
358	0.0	5.84375	32.4375
359	0.0	11.6875	32.4375
360	0.0	17.5313	32.4375
361	0.0	23.375	32.4375
362	0.0	-23.375	26.5938
363	0.0	-17.5313	26.5938
364	0.0	-11.6875	26.5938
365	0.0	-5.84375	26.5938
366	0.0	0.0	26.5938
367	0.0	5.84375	26.5938
368	0.0	11.6875	26.5938
369	0.0	17.5313	26.5938
370	0.0	23.375	26.5938
371	0.0	-23.375	20.7500
372	0.0	-17.5313	20.7500
373	0.0	-11.6875	20.7500
374	0.0	-5.84375	20.7500
375	0.0	0.0	20.7500
376	0.0	5.84375	20.7500
377	0.0	11.6875	20.7500
378	0.0	17.5313	20.7500
379	0.0	23.375	20.7500

Joint No.	Radial (in.)	Circumferential (deg.)	Global 3 (in.)
380	3.250	0.0	10.350
381	3.250	22.5	10.350
382	3.250	0.0	8.200
383	3.250	22.5	8.200
384	3.250	45.0	8.200
385	3.250	67.5	8.200
386	3.250	90.0	8.200
387	3.250	112.5	8.200
388	3.250	135.0	8.200
389	3.250	157.5	8.200
390	3.250	180.0	8.200
391	3.250	202.5	8.200
392	3.250	225.0	8.200
393	3.250	247.5	8.200
394	3.250	270.0	8.200
395	3.250	292.5	8.200
396	3.250	315.0	8.200

Joint No.	Radial (in.)	Circumferential (deg.)	Global 3 (in.)
397	3.250	337.5	8.200
398	3.250	0.0	6.400
399	3.250	22.5	6.400
400	3.250	45.0	6.400
401	3.250	67.5	6.400
402	3.250	90.0	6.400
403	3.250	112.5	6.400
404	3.250	135.0	6.400
405	3.250	157.5	6.400
406	3.250	180.0	6.400
407	3.250	202.5	6.400
408	3.250	225.0	6.400
409	3.250	247.5	6.400
410	3.250	270.0	6.400
411	3.250	292.5	6.400
412	3.250	315.0	6.400
413	3.250	337.5	6.400

Joint No.	Global 1 (in.)	Global 2 (in.)	Global 3 (in.)
478	6.40	-6.40	-6.40
479	6.40	-3.20	-6.40
480	6.40	0.0	-6.40
481	6.40	3.20	-6.40
482	6.40	6.40	-6.40
483	3.20	6.40	-6.40
484	0.0	6.40	-6.40
485	-3.20	6.40	-6.40
486	-6.40	6.40	-6.40
487	-6.40	3.20	-6.40
488	-6.40	0.0	-6.40
489	-6.40	-3.20	-6.40
490	-6.40	-6.40	-6.40
491	-3.20	-6.40	-6.40
492	0.0	-6.40	-6.40
493	3.20	-6.40	-6.40
494	6.40	-6.40	6.40
495	6.40	-3.20	6.40
496	6.40	0.0	6.40
497	6.40	3.20	6.40
498	6.40	6.40	6.40
499	3.20	6.40	6.40
500	0.0	6.40	6.40
501	-3.20	6.40	6.40
502	-6.40	6.40	6.40
503	-6.40	3.20	6.40
504	-6.40	0.0	6.40
505	-6.40	-3.20	6.40
506	-6.40	-6.40	6.40

Joint No.	Global 1 (in.)	Global 2 (in.)	Global 3 (in.)
507	-3.20	-6.40	6.40
508	0.0	-6.40	6.40
509	3.20	-6.40	6.40
510	6.40	6.40	-3.20
511	6.40	6.40	0.0
512	6.40	6.40	3.20
513	6.40	-6.40	3.20
514	6.40	-6.40	0.0
515	6.40	-6.40	-3.20
516	-6.40	6.40	3.20
517	-6.40	6.40	0.0
518	-6.40	6.40	-3.20
519	-6.40	-6.40	-3.20
520	-6.40	-6.40	0.0
521	-6.40	-6.40	3.20

Joint No.	Radial (in.)	Circumferential (deg.)	Global 3 (in.)
614	3.250	45.0	10.350
615	3.250	67.5	10.350
616	3.250	90.0	10.350
617	3.250	112.5	10.350
618	3.250	135.0	10.350
619	3.250	157.5	10.350
620	3.250	180.0	10.350
621	3.250	202.5	10.350
622	3.250	225.0	10.350
623	3.250	247.5	10.350
624	3.250	270.0	10.350
625	3.250	292.5	10.350
626	3.250	315.0	10.350
627	3.250	337.5	10.350

TABLE 2. JOINT LOCATIONS IN RIGHT COORDINATE SYSTEM
(includes right solar panel grid points)

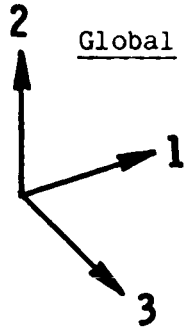

Global

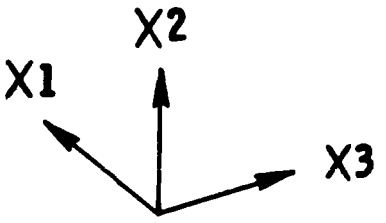

Right Side
(90 deg. about 2)

Joint No.	Radial (in.)	Circumferential (deg.)	X3 (in.)
3	0.0	0.0	15.080
Joint No.	X1(in)	X2(in)	X3(in)
177	-12.62	0.0	124.26
178	0.0	0.0	124.26
179	12.62	0.0	124.26
180	-12.62	0.0	111.75
181	0.0	0.0	111.75
182	12.62	0.0	111.75
183	-12.62	0.0	99.24
184	0.0	0.0	99.24
185	12.62	0.0	99.24
186	-12.62	0.0	86.73
187	0.0	0.0	86.73
188	12.62	0.0	86.73
189	-12.62	0.0	74.22
190	0.0	0.0	74.22
191	12.62	0.0	74.22
192	-12.62	0.0	61.71
193	0.0	0.0	61.71
194	12.62	0.0	61.71
195	-12.62	0.0	49.20
196	0.0	0.0	49.20
197	12.62	0.0	49.20
198	-12.62	0.0	36.52
199	0.0	0.0	36.52
200	12.62	0.0	36.52
201	-12.62	0.0	23.83
202	0.0	0.0	23.83
203	12.62	0.0	23.83
204	-2.75	0.0	12.42
205	2.75	0.0	12.42

Joint No.	Radial (in.)	Circumferential (deg.)	X3 (in.)
206	3.250	0.0	8.200
207	3.250	22.5	8.200
208	3.250	45.0	8.200
209	3.250	67.5	8.200
210	3.250	90.0	8.200
211	3.250	112.5	8.200
212	3.250	135.0	8.200
213	3.250	157.5	8.200
214	3.250	180.0	8.200
215	3.250	202.5	8.200
216	3.250	225.0	8.200
217	3.250	247.5	8.200
218	3.250	270.0	8.200
219	3.250	292.5	8.200
220	3.250	315.0	8.200
221	3.250	337.5	8.200
222	3.250	0.0	6.400
223	3.250	22.5	6.400
224	3.250	45.0	6.400
225	3.250	67.5	6.400
226	3.250	90.0	6.400
227	3.250	112.5	6.400
228	3.250	135.0	6.400
229	3.250	157.5	6.400
230	3.250	180.0	6.400
231	3.250	202.5	6.400
232	3.250	225.0	6.400
233	3.250	247.5	6.400
234	3.250	270.0	6.400
235	3.250	292.5	6.400
236	3.250	315.0	6.400
237	3.250	337.5	6.400
522	3.625	0.0	12.420
523	3.625	22.5	12.420
524	3.625	45.0	12.420
525	3.625	67.5	12.420
526	3.625	90.0	12.420
527	3.625	112.5	12.420
528	3.625	135.0	12.420
529	3.625	157.5	12.420
530	3.625	180.0	12.420
531	3.625	202.5	12.420
532	3.625	225.0	12.420
533	3.625	247.5	12.420
534	3.625	270.0	12.420
535	3.625	292.5	12.420
536	3.625	315.0	12.420
537	3.625	337.5	12.420

Joint No.	X1(in)	X2(in)	X3(in)
538	0.0	-1.75	12.42
539	0.0	0.0	12.42
540	0.0	1.75	12.42
541	-7.45	0.0	12.89
542	7.45	0.0	12.89
543	-11.75	0.0	12.89
544	-7.45	0.0	15.08
545	-7.45	0.0	15.08
546	7.45	0.0	15.08
547	7.45	0.0	15.08
548	-11.75	0.0	15.08
549	-11.75	0.0	15.08
550	-3.275	0.0	15.08
551	3.275	0.0	15.08

Joint No.	Radial (in.)	Circumferential (deg.)	X3 (in.)
582	3.625	0.0	8.200
583	3.625	22.5	8.200
584	3.625	45.0	8.200
585	3.625	67.5	8.200
586	3.625	90.0	8.200
587	3.625	112.5	8.200
588	3.625	135.0	8.200
589	3.625	157.5	8.200
590	3.625	180.0	8.200
591	3.625	202.5	8.200
592	3.625	225.0	8.200
593	3.625	247.5	8.200
594	3.625	270.0	8.200
595	3.625	292.5	8.200
596	3.625	315.0	8.200
597	3.625	337.5	8.200

Joint No.	X1(in)	X2(in)	X3(in)
628	-12.62	0.0	174.30
629	0.0	0.0	174.30
630	12.62	0.0	174.30
631	-12.62	0.0	161.79
632	0.0	0.0	161.79
633	12.62	0.0	161.79
634	-12.62	0.0	149.28
635	0.0	0.0	149.28
636	12.62	0.0	149.28
637	-12.62	0.0	136.77
638	0.0	0.0	136.77
639	12.62	0.0	136.77
652	-582.73	0.0	49.25

TABLE 3. JOINT LOCATIONS IN LEFT COORDINATE SYSTEM
(includes left solar panel grid points)

Global

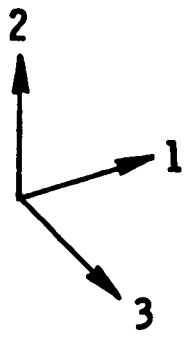

Left Side
(-90 deg. about 2)

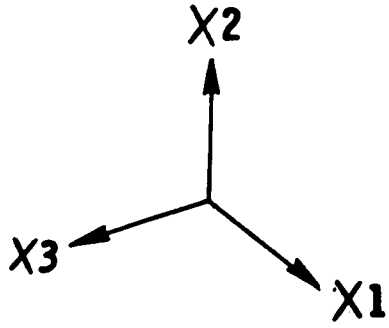

Joint No.	Radial (in.)	Circumferential (deg.)	X3 (in.)
4	0.0	0.0	15.080
Joint No.	**X1(in)**	**X2(in)**	**X3(in)**
238	-12.62	0.0	124.26
239	0.0	0.0	124.26
240	12.62	0.0	124.26
241	-12.62	0.0	111.75
242	0.0	0.0	111.75
243	12.62	0.0	111.75
244	-12.62	0.0	99.24
245	0.0	0.0	99.24
246	12.62	0.0	99.24
247	-12.62	0.0	86.73
248	0.0	0.0	86.73
249	12.62	0.0	86.73
250	-12.62	0.0	74.22
251	0.0	0.0	74.22
252	12.62	0.0	74.22
253	-12.62	0.0	61.71
254	0.0	0.0	61.71
255	12.62	0.0	61.71
256	-12.62	0.0	49.20
257	0.0	0.0	49.20
258	12.62	0.0	49.20
259	-12.62	0.0	36.52
260	0.0	0.0	36.52
261	12.62	0.0	36.52
262	-12.62	0.0	23.83
263	0.0	0.0	23.83
264	12.62	0.0	23.83
265	-2.75	0.0	12.42
266	2.75	0.0	12.42
267	3.250	0.0	8.200
268	3.250	22.5	8.200

Joint No.	Radial (in.)	Circumferential (deg.)	X3 (in.)
269	3.250	45.0	8.200
270	3.250	67.5	8.200
271	3.250	90.0	8.200
272	3.250	112.5	8.200
273	3.250	135.0	8.200
274	3.250	157.5	8.200
275	3.250	180.0	8.200
276	3.250	202.5	8.200
277	3.250	225.0	8.200
278	3.250	247.5	8.200
279	3.250	270.0	8.200
280	3.250	292.5	8.200
281	3.250	315.0	8.200
282	3.250	337.5	8.200
283	3.250	0.0	6.400
284	3.250	22.5	6.400
285	3.250	45.0	6.400
286	3.250	67.5	6.400
287	3.250	90.0	6.400
288	3.250	112.5	6.400
289	3.250	135.0	6.400
290	3.250	157.5	6.400
291	3.250	180.0	6.400
292	3.250	202.5	6.400
293	3.250	225.0	6.400
294	3.250	247.5	6.400
295	3.250	270.0	6.400
296	3.250	292.5	6.400
297	3.250	315.0	6.400
298	3.250	337.5	6.400
552	3.625	0.0	12.420
553	3.625	22.5	12.420
554	3.625	45.0	12.420
555	3.625	67.5	12.420
556	3.625	90.0	12.420
557	3.625	112.5	12.420
558	3.625	135.0	12.420
559	3.625	157.5	12.420
560	3.625	180.0	12.420
561	3.625	202.5	12.420
562	3.625	225.0	12.420
563	3.625	247.5	12.420
564	3.625	270.0	12.420
565	3.625	292.5	12.420
566	3.625	315.0	12.420
567	3.625	337.5	12.420

Joint No.	X1(in)	X2(in)	X3(in)
568	0.0	-1.75	12.42
569	0.0	0.0	12.42
570	0.0	1.75	12.42
571	-7.45	0.0	12.89
572	7.45	0.0	12.89
573	11.75	0.0	12.89
574	-7.45	0.0	15.08
575	-7.45	0.0	15.08
576	7.45	0.0	15.08
577	7.45	0.0	15.08
578	11.75	0.0	15.08
579	11.75	0.0	15.08
580	-3.275	0.0	15.08
581	3.275	0.0	15.08

Joint No.	Radial (in.)	Circumferential (deg.)	X3 (in.)
598	3.625	0.0	8.200
599	3.625	22.5	8.200
600	3.625	45.0	8.200
601	3.625	67.5	8.200
602	3.625	90.0	8.200
603	3.625	112.5	8.200
604	3.625	135.0	8.200
605	3.625	157.5	8.200
606	3.625	180.0	8.200
607	3.625	202.5	8.200
608	3.625	225.0	8.200
609	3.625	247.5	8.200
610	3.625	270.0	8.200
611	3.625	292.5	8.200
612	3.625	315.0	8.200
613	3.625	337.5	8.200

Joint No.	X1(in)	X2(in)	X3(in)
640	-12.62	0.0	174.30
641	0.0	0.0	174.30
642	12.62	0.0	174.30
643	-12.62	0.0	161.79
644	0.0	0.0	161.79
645	12.62	0.0	161.79
646	-12.62	0.0	149.28
647	0.0	0.0	149.28
648	12.62	0.0	149.28
649	-12.62	0.0	136.77
650	0.0	0.0	136.77
651	12.62	0.0	136.77
653	582.73	0.0	49.25

TABLE 4. JOINT LOCATIONS IN TOP COORDINATE SYSTEM

Global

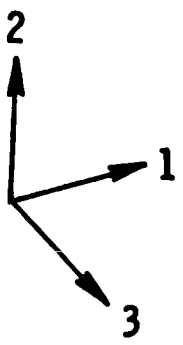

Top
(-90 deg. about 1)

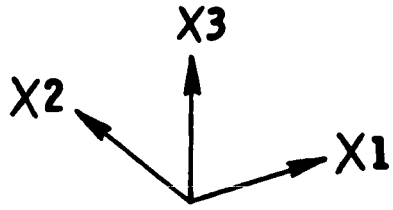

Joint No.	Radial (in.)	Circumferential (deg.)	X3 (in.)
414	3.250	0.0	8.200
415	3.250	22.5	8.200
416	3.250	45.0	8.200
417	3.250	67.5	8.200
418	3.250	90.0	8.200
419	3.250	112.5	8.200
420	3.250	135.0	8.200
421	3.250	157.5	8.200
422	3.250	180.0	8.200
423	3.250	202.5	8.200
424	3.250	225.0	8.200
425	3.250	247.5	8.200
426	3.250	270.0	8.200
427	3.250	292.5	8.200
428	3.250	315.0	8.200
429	3.250	337.5	8.200
430	3.250	0.0	6.400
431	3.250	22.5	6.400
432	3.250	45.0	6.400
433	3.250	67.5	6.400
434	3.250	90.0	6.400
435	3.250	112.5	6.400
436	3.250	135.0	6.400
437	3.250	157.5	6.400
438	3.250	180.0	6.400
439	3.250	202.5	6.400
440	3.250	225.0	6.400
441	3.250	247.5	6.400
442	3.250	270.0	6.400
443	3.250	292.5	6.400
444	3.250	315.0	6.400
445	3.250	337.5	6.400

TABLE 5. JOINT LOCATIONS IN BOTTOM COORDINATE SYSTEM

Global

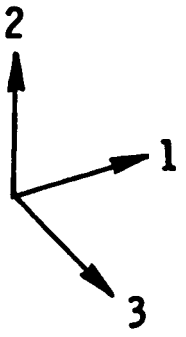

Bottom
(90 deg. about 1)

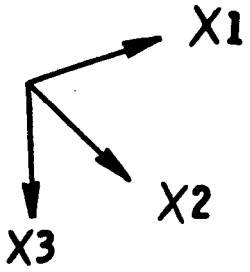

Joint No.	Radial (in.)	Circumferential (deg.)	X3 (in.)
446	3.250	0.0	8.200
447	3.250	22.5	8.200
448	3.250	45.0	8.200
449	3.250	67.5	8.200
450	3.250	90.0	8.200
451	3.250	112.5	8.200
452	3.250	135.0	8.200
453	3.250	157.5	8.200
454	3.250	180.0	8.200
455	3.250	202.5	8.200
456	3.250	225.0	8.200
457	3.250	247.5	8.200
458	3.250	270.0	8.200
459	3.250	292.5	8.200
460	3.250	315.0	8.200
461	3.250	337.5	8.200
462	3.250	0.0	6.400
463	3.250	22.5	6.400
464	3.250	45.0	6.400
465	3.250	67.5	6.400
466	3.250	90.0	6.400
467	3.250	112.5	6.400
468	3.250	135.0	6.400
469	3.250	157.5	6.400
470	3.250	180.0	6.400
471	3.250	202.5	6.400
472	3.250	225.0	6.400
473	3.250	247.5	6.400
474	3.250	270.0	6.400
475	3.250	292.5	6.400
476	3.250	315.0	6.400
477	3.250	337.5	6.400

TABLE 6. COMPARISON OF LEFT AND RIGHT SOLAR ARRAY GRID POINT NUMBERS

Right Solar Array Grid Points	Left Solar Array Grid Points	Difference (left-right)
3	4	1
177 to 237	238 to 298	61
522 to 551	552 to 581	30
582 to 597	598 to 613	16
628 to 652	640 to 653	12

NOTE:

1. This table shows the difference in grid point numbers in the right solar array, Table 2, and the left solar array, Table 3.

2. All of the grid point local coordinates are identical in Table 2 and Table 3 except the left solar array grid point numbers 573,578 and 579 have a local X1 dimension of -11.75 compared to the +11.75 X1 dimension used in the corresponding right solar array grid point numbers 543,548 and 549.

Table 7. Measured and Predicted Model Weights

Substructure		Analysis (lbs.)	Measured (lbs.)
Habitation Module	plates	16.931	
	beams	4.703	
	lumped mass	2.530	
Total		24.164	23.9
Connecting Cube	plates	8.090	
	beams	9.896	
Total		17.986	17.6
Radiator	plates	12.620	
	beams	15.484	
Total		28.104	27.2
Right Solar Array	motor	8.010	
	bearings	6.380	
	plates	26.264	
	beams	22.446	
Total		63.100	63.1
Left Solar Array			
Total		63.100	63.1
Total Substructure Weight		196.454	194.9

Table 8. Center of Gravity and Mass Inertia Properties

Model	Global Coordinate (in.) X	Y	Z	Mass Inertia ($lb\text{-}s^2/in$) Ix	Iy	Iz
Habitation Module	0.0	0.0	-42.506	29.513	29.513	8.180
Connecting Cube	0.0	0.0	0.0	2.22	2.22	2.22
Radiator	0.0	0.0	28.535	33.812	24.181	9.935
Right Solar Array	54.26	0.0	1.915	9.741	441.6	432.01
Left Solar Array	-54.26	0.0	1.915	9.741	441.6	432.01
Assemblage	0.0	0.0	0.334	261.42	2073.6	1842.5

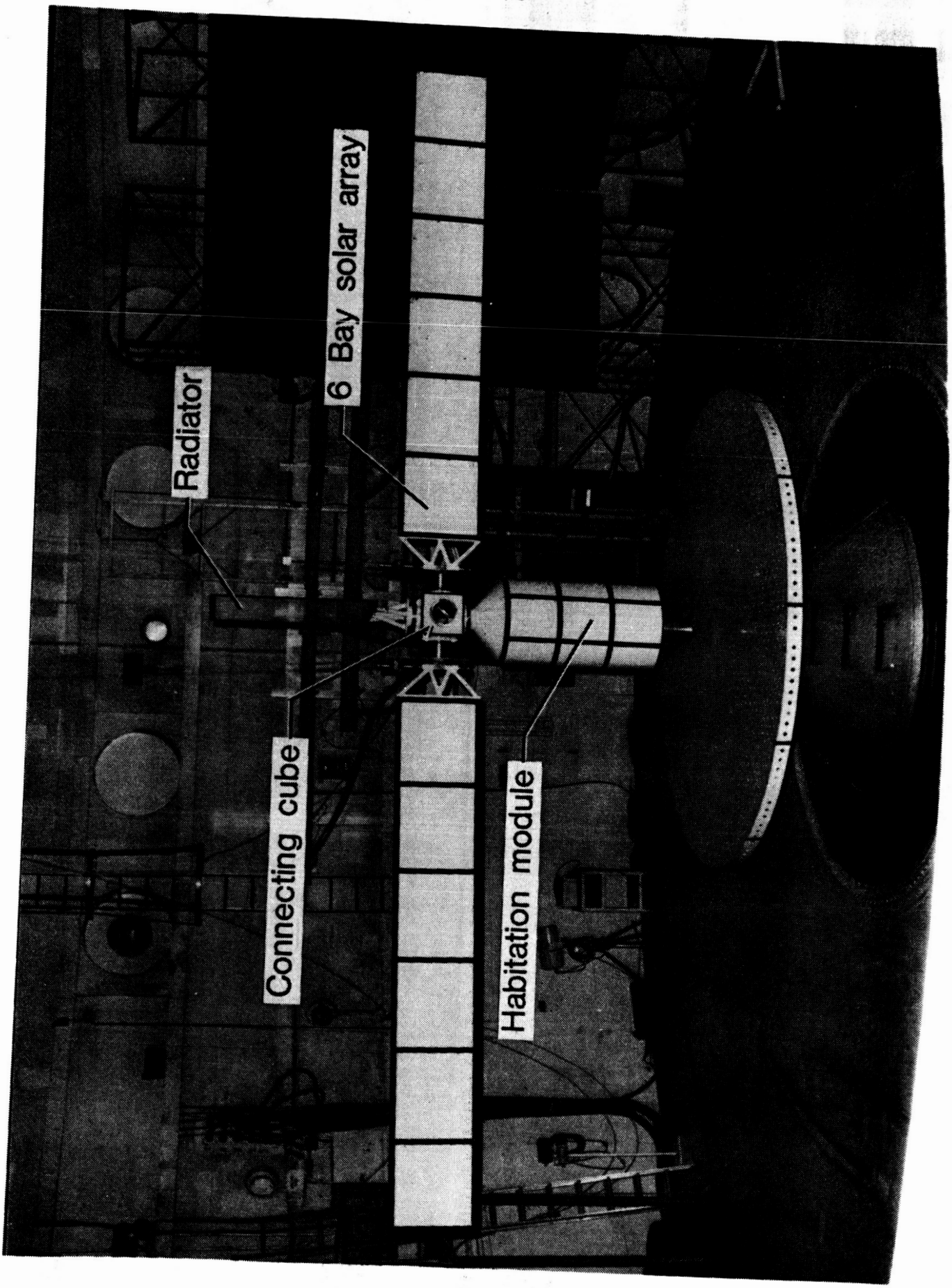

Figure 1. Experimental Generic Dynamic Model

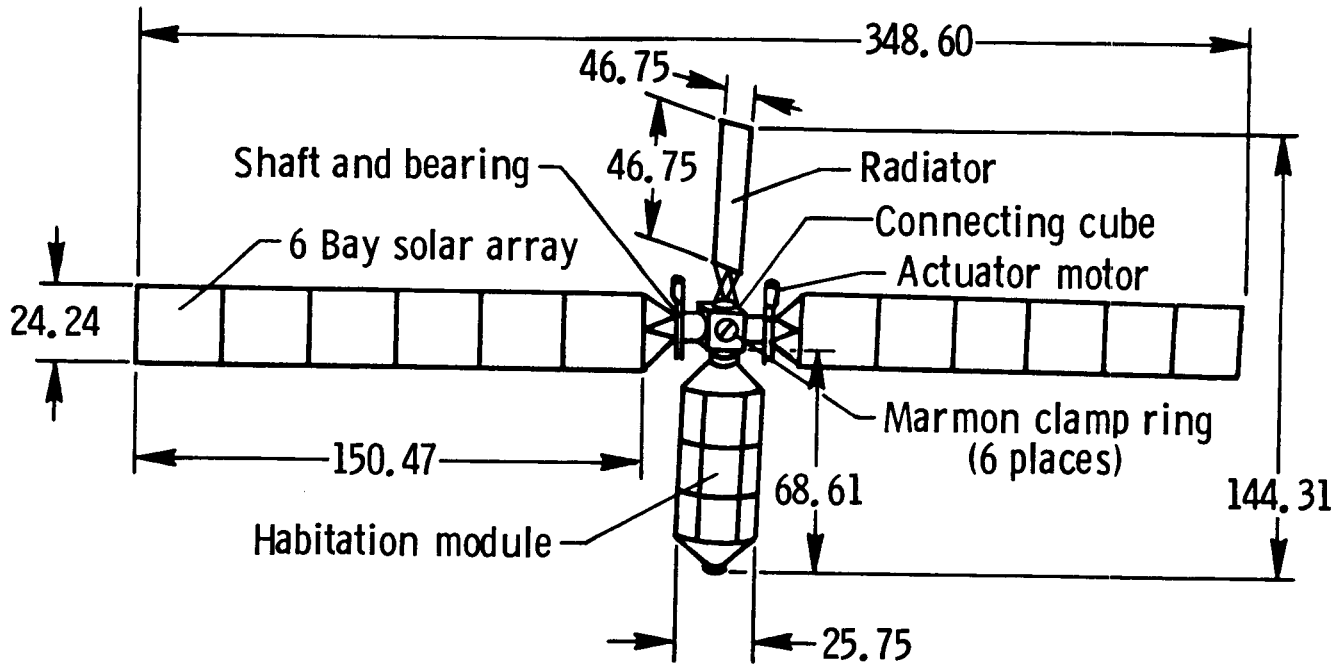

Figure 2. Experimental Generic Model Dimensions

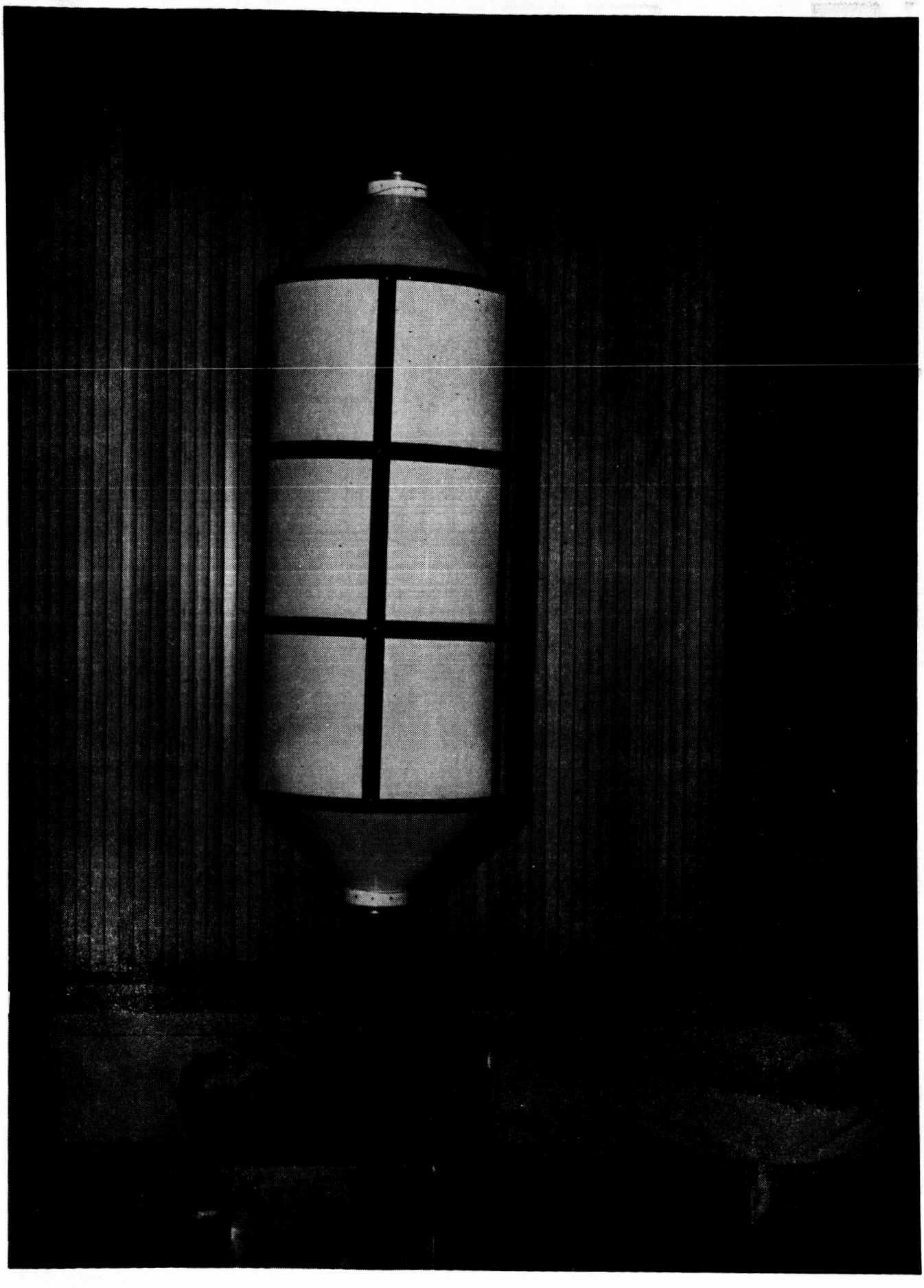

Figure 3. Habitation Module

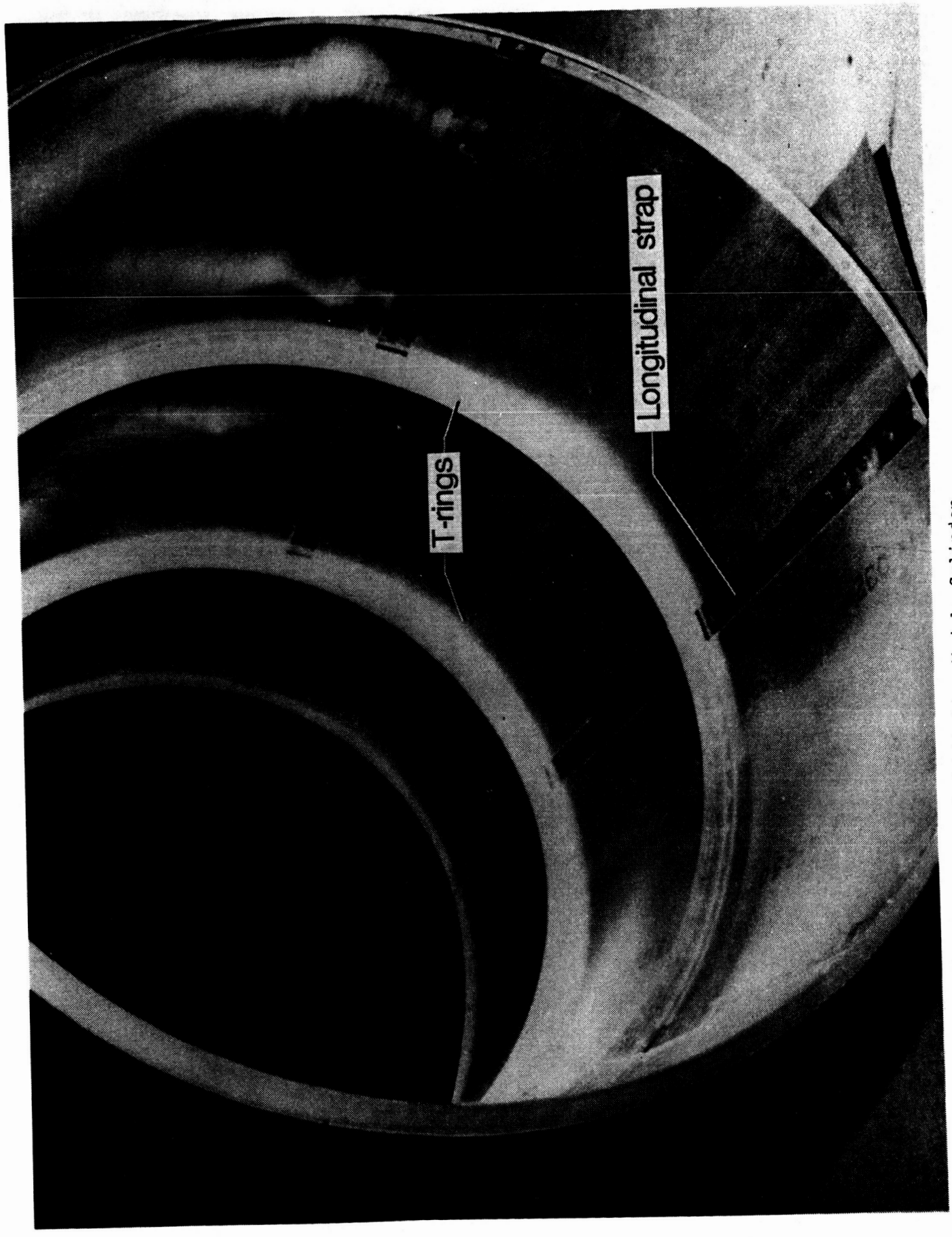

Figure 4. Internal View of Habitation Module Cylinder

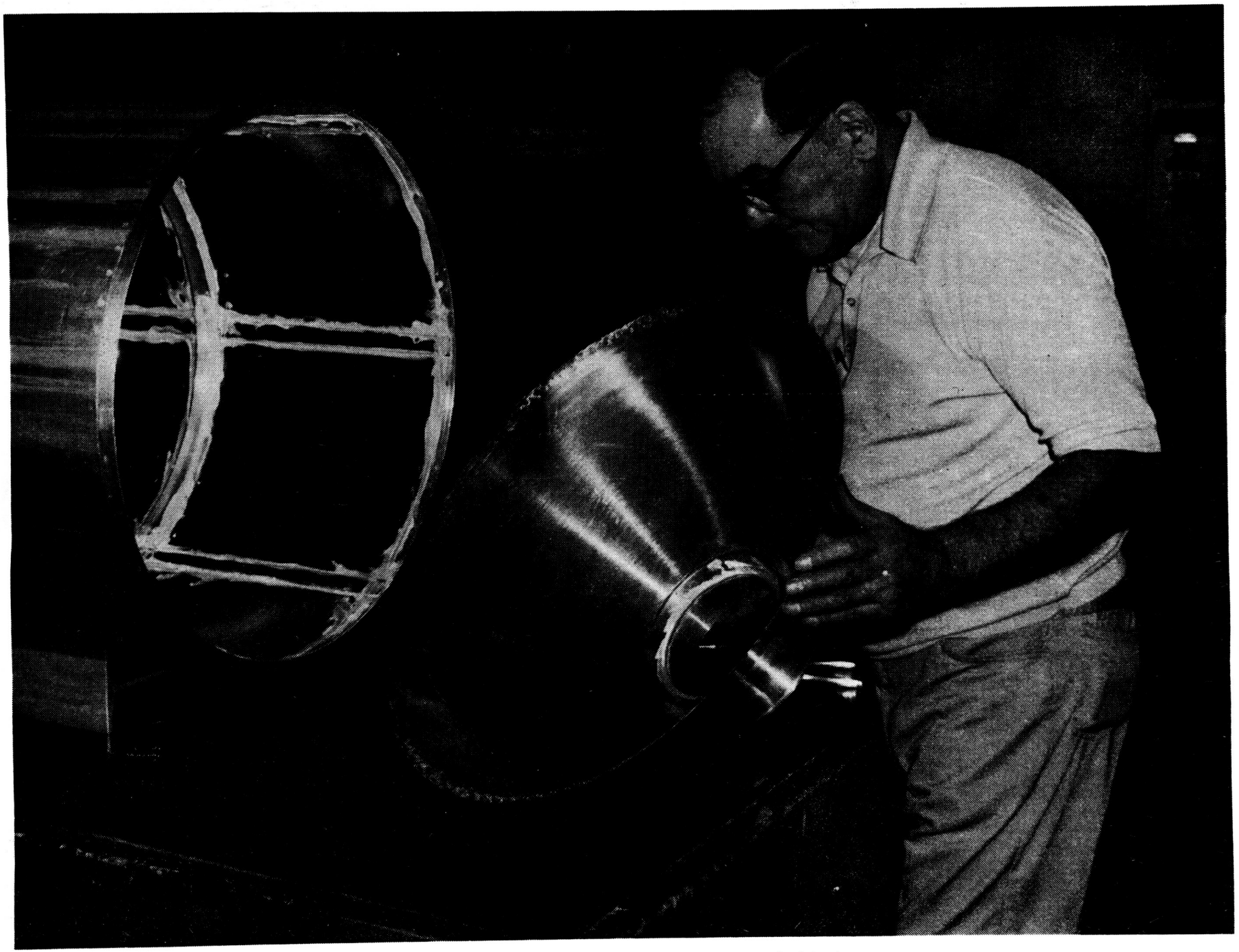

Figure 5. Mating of Conical End Section to Habitation Module Cylinder

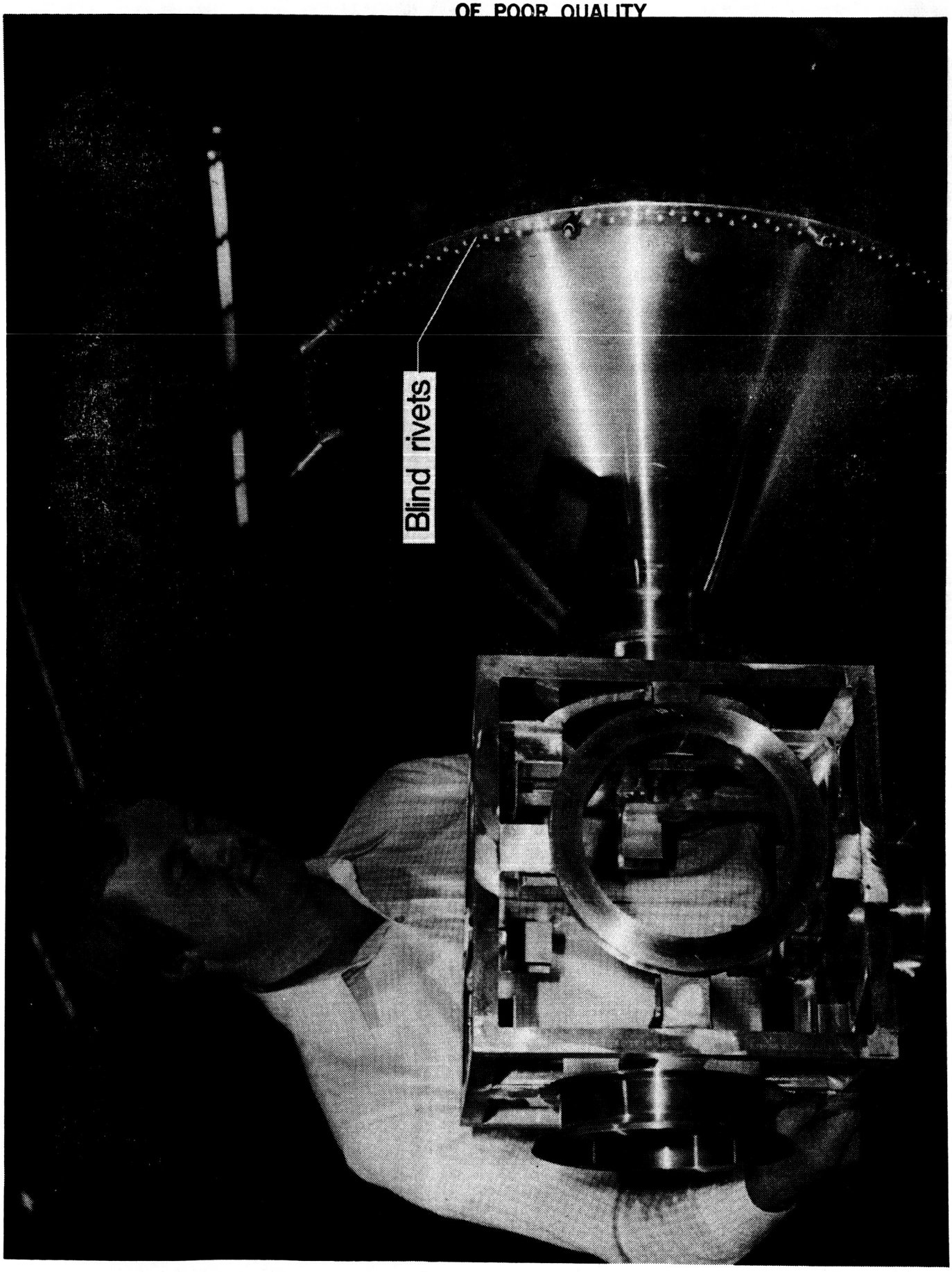

Figure 6. Fabrication of Connecting Cube and Habitation Module

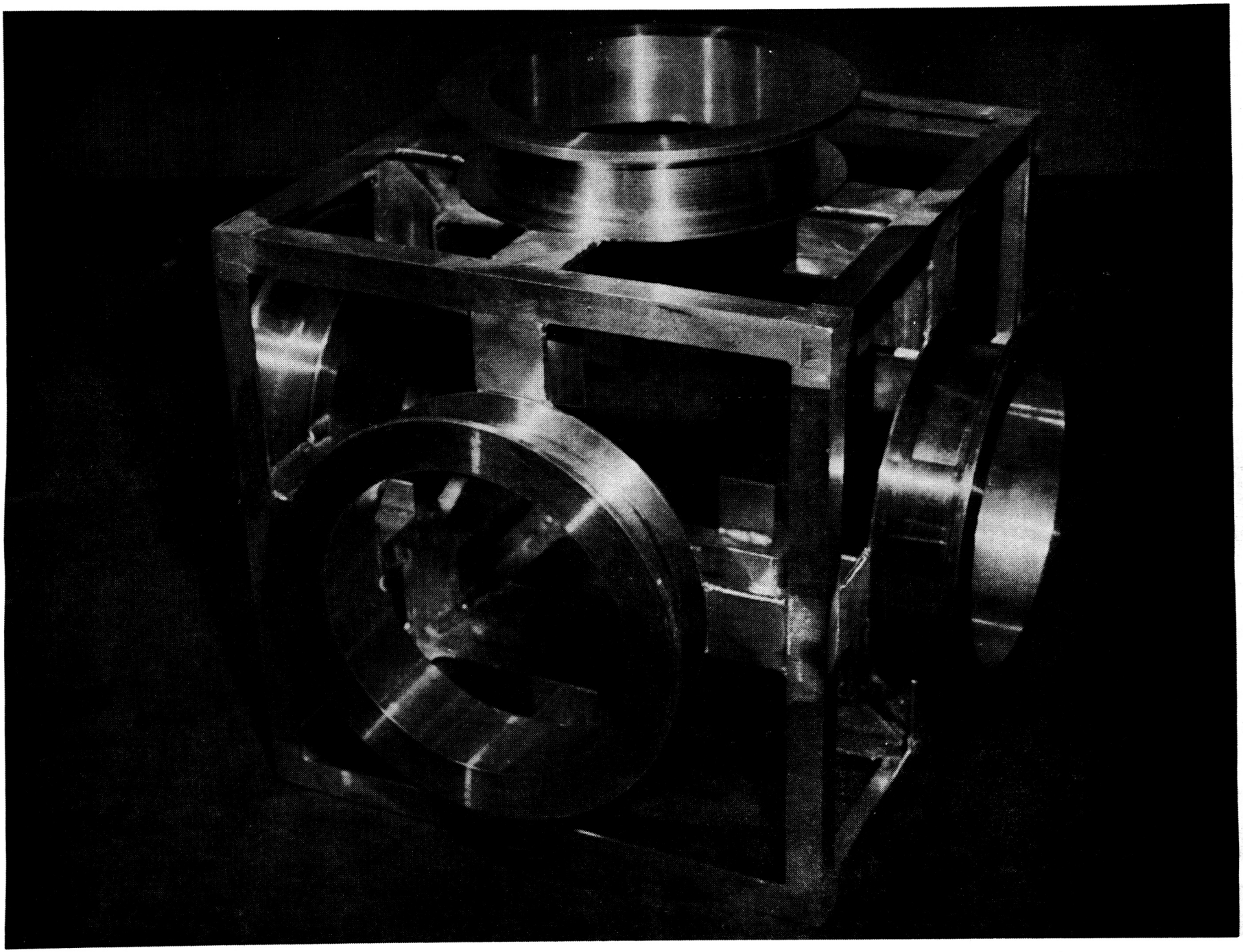

Figure 7. Connecting Cube Framework

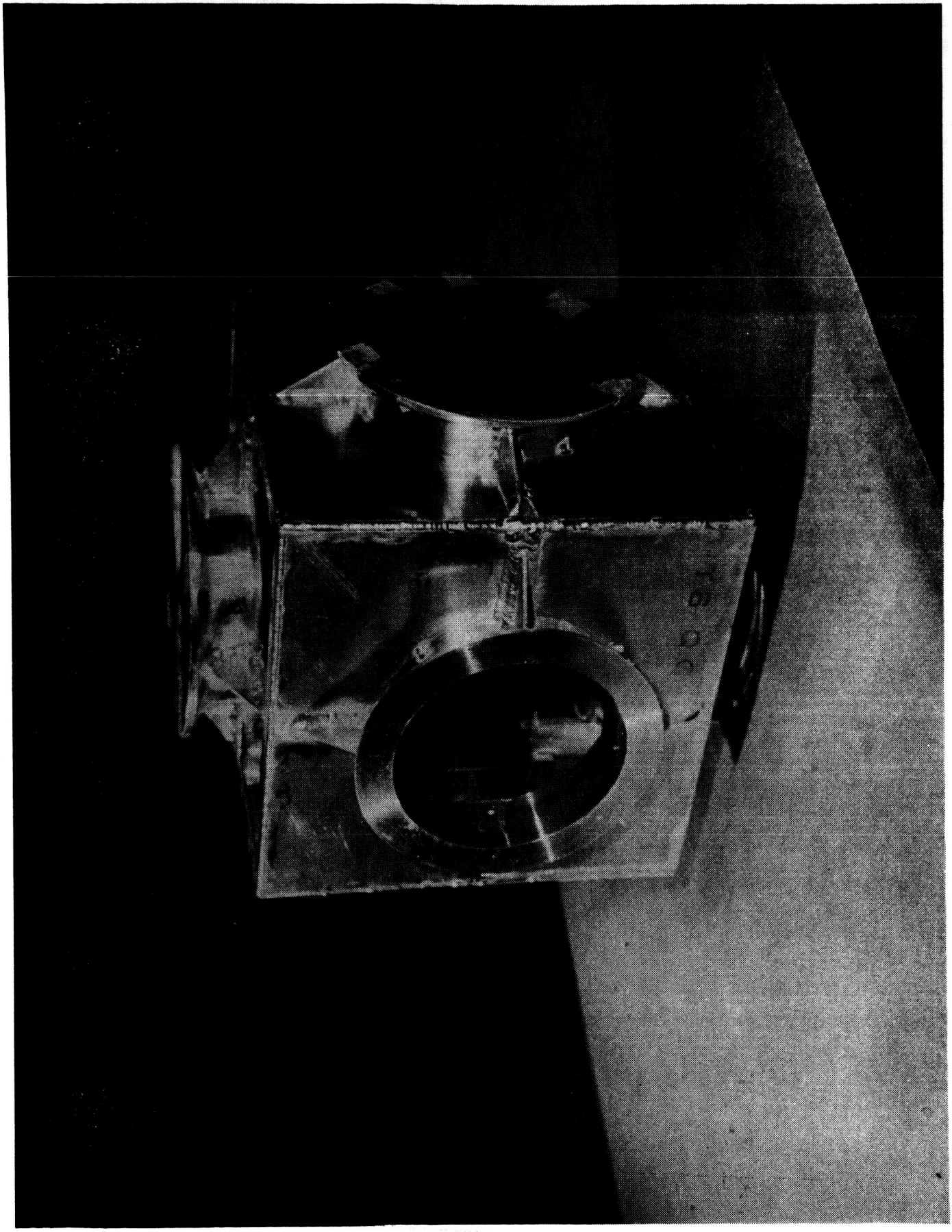

Figure 8. Connecting Cube With Skin and Triangular Stiffeners

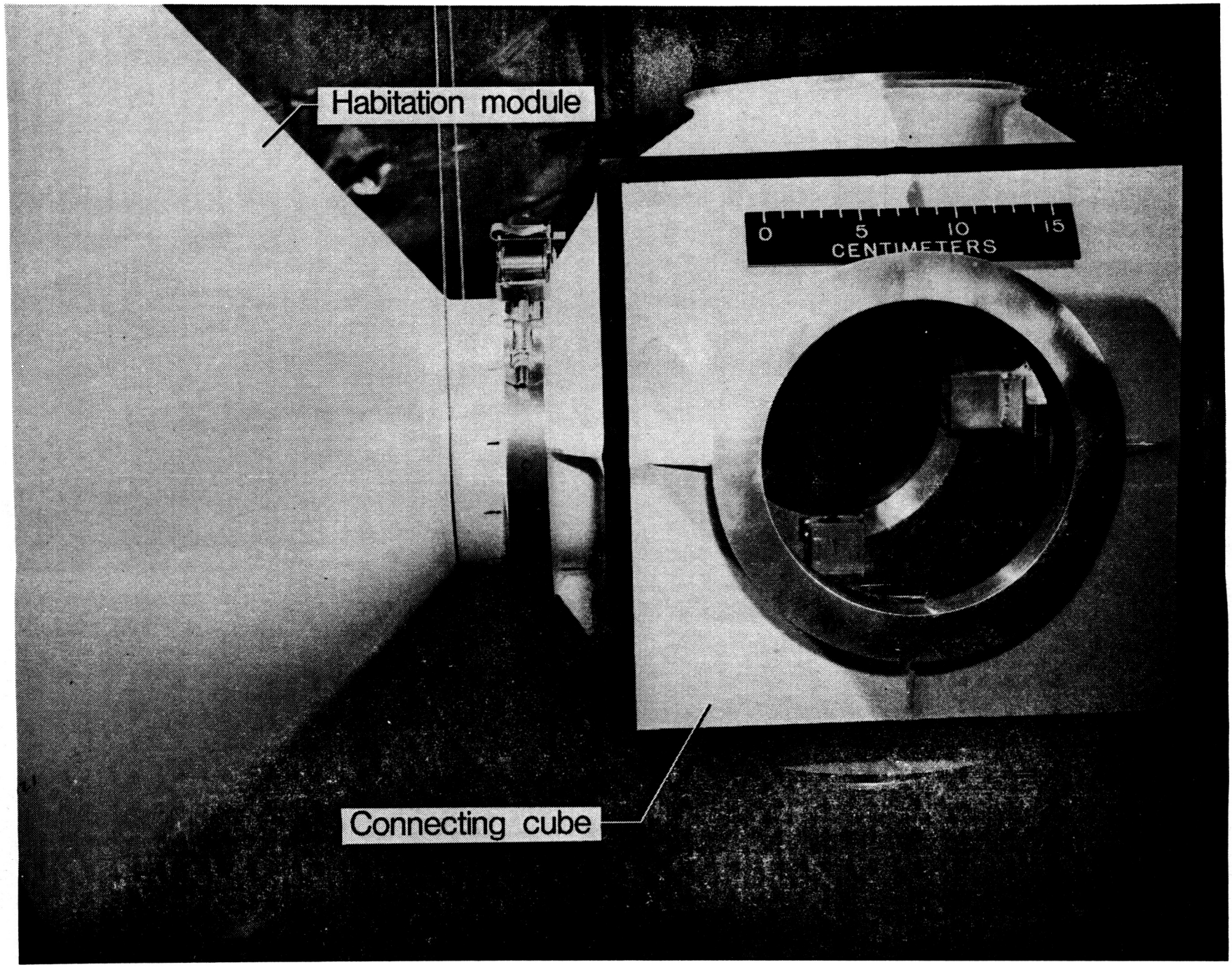

Figure 9. Connecting Cube Mated to Habitation Module

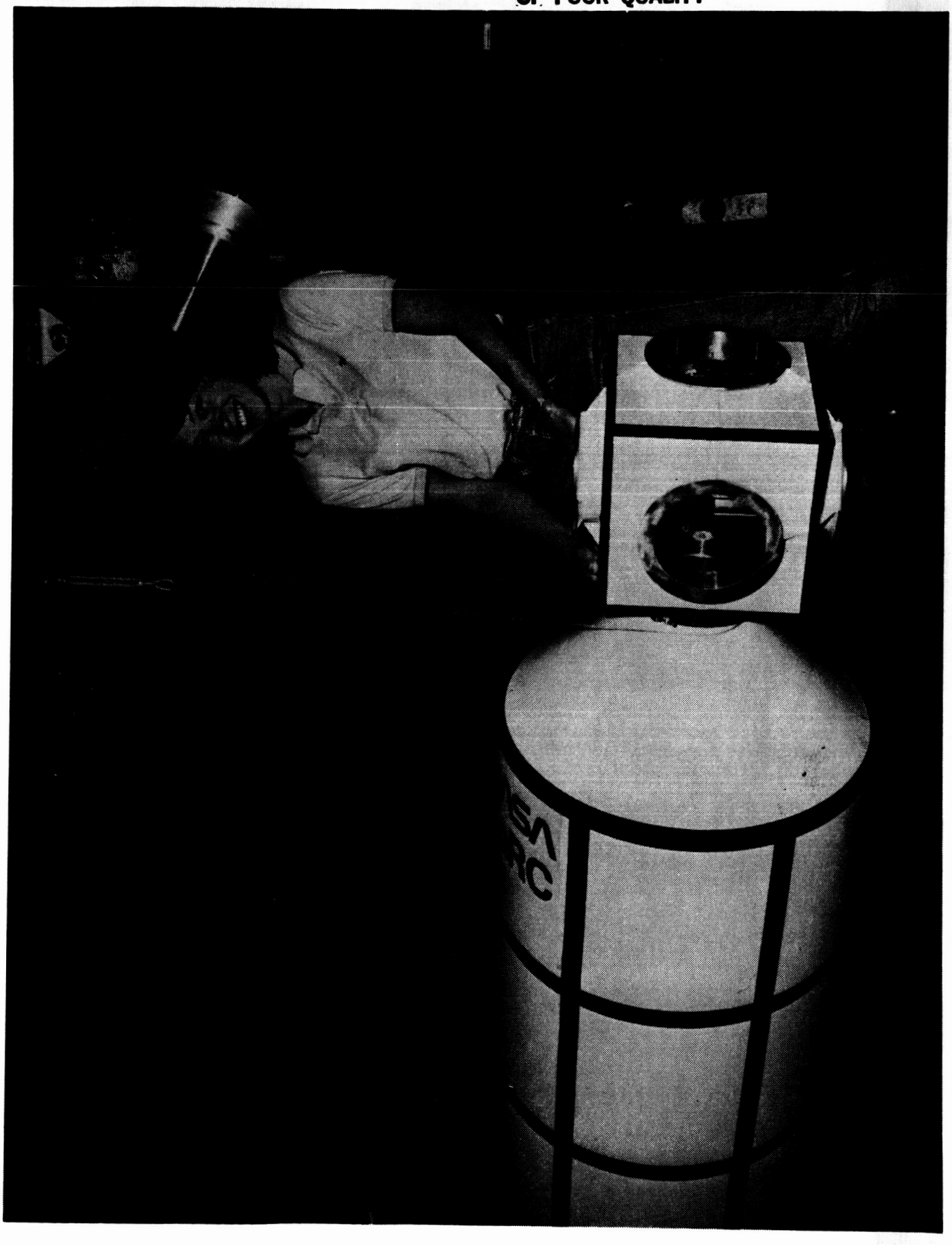

Figure 10. Relative Size of Connecting Cube and Habitation Module

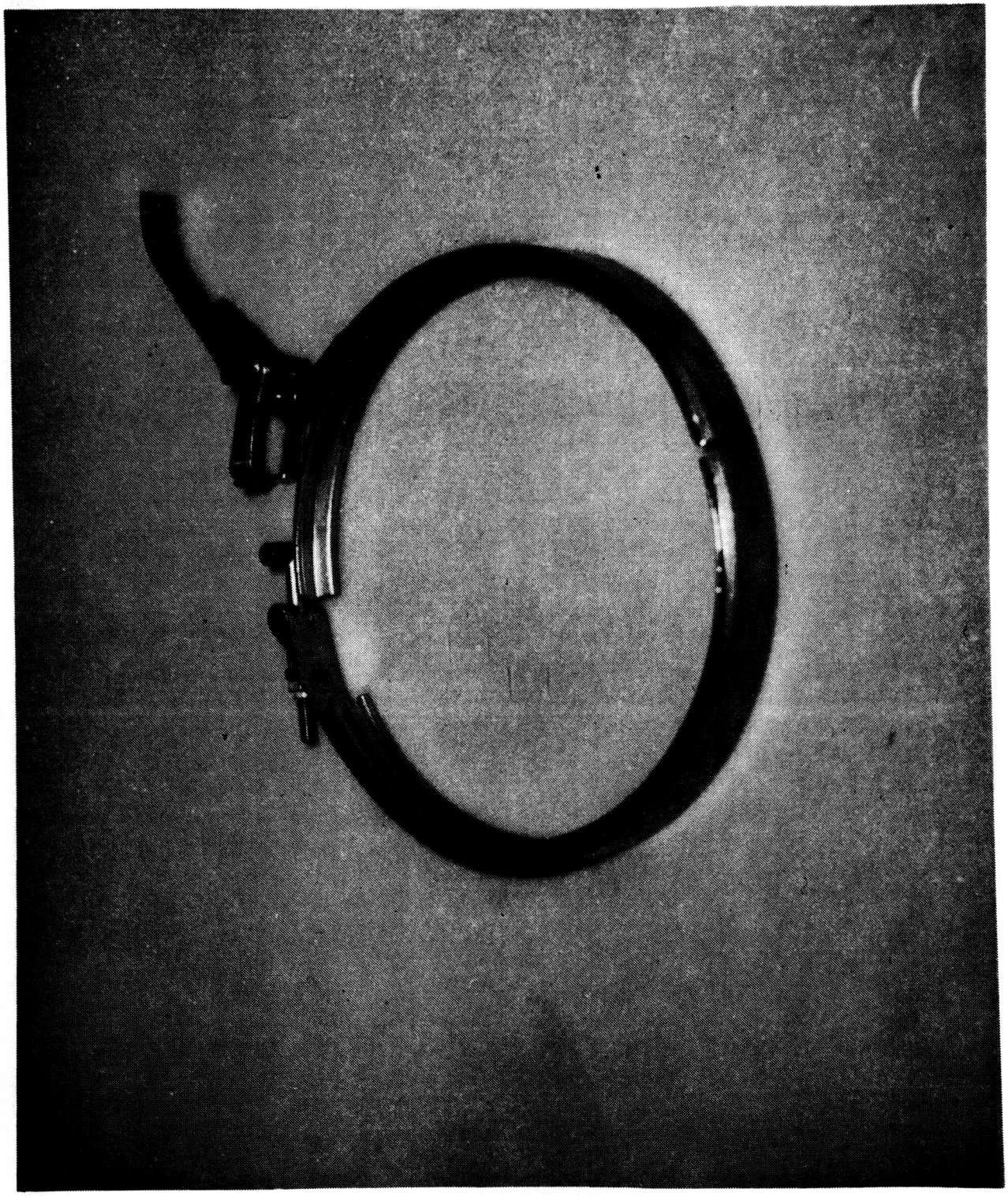

Figure 11. Marmon Clamp

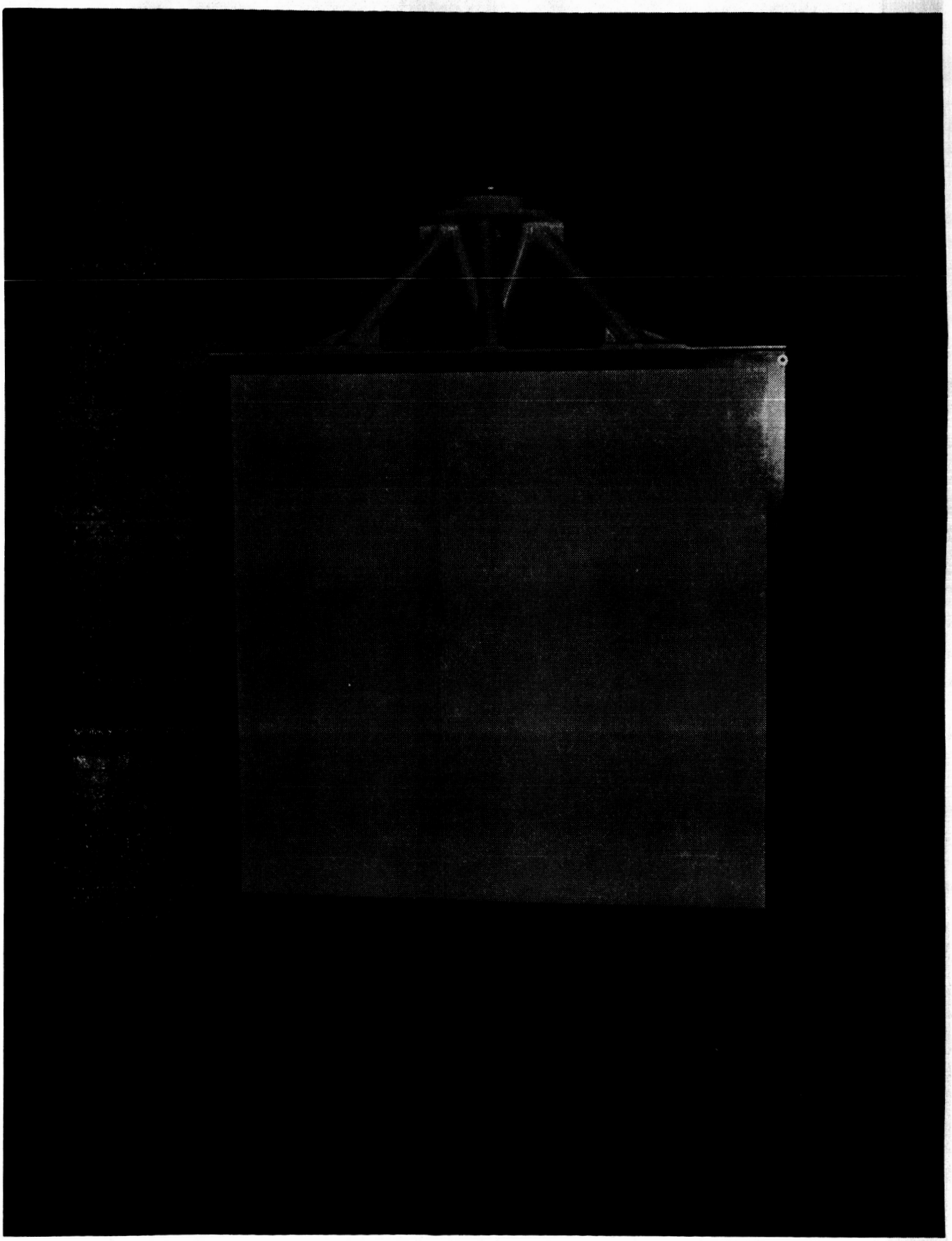

Figure 12. Radiator Panel

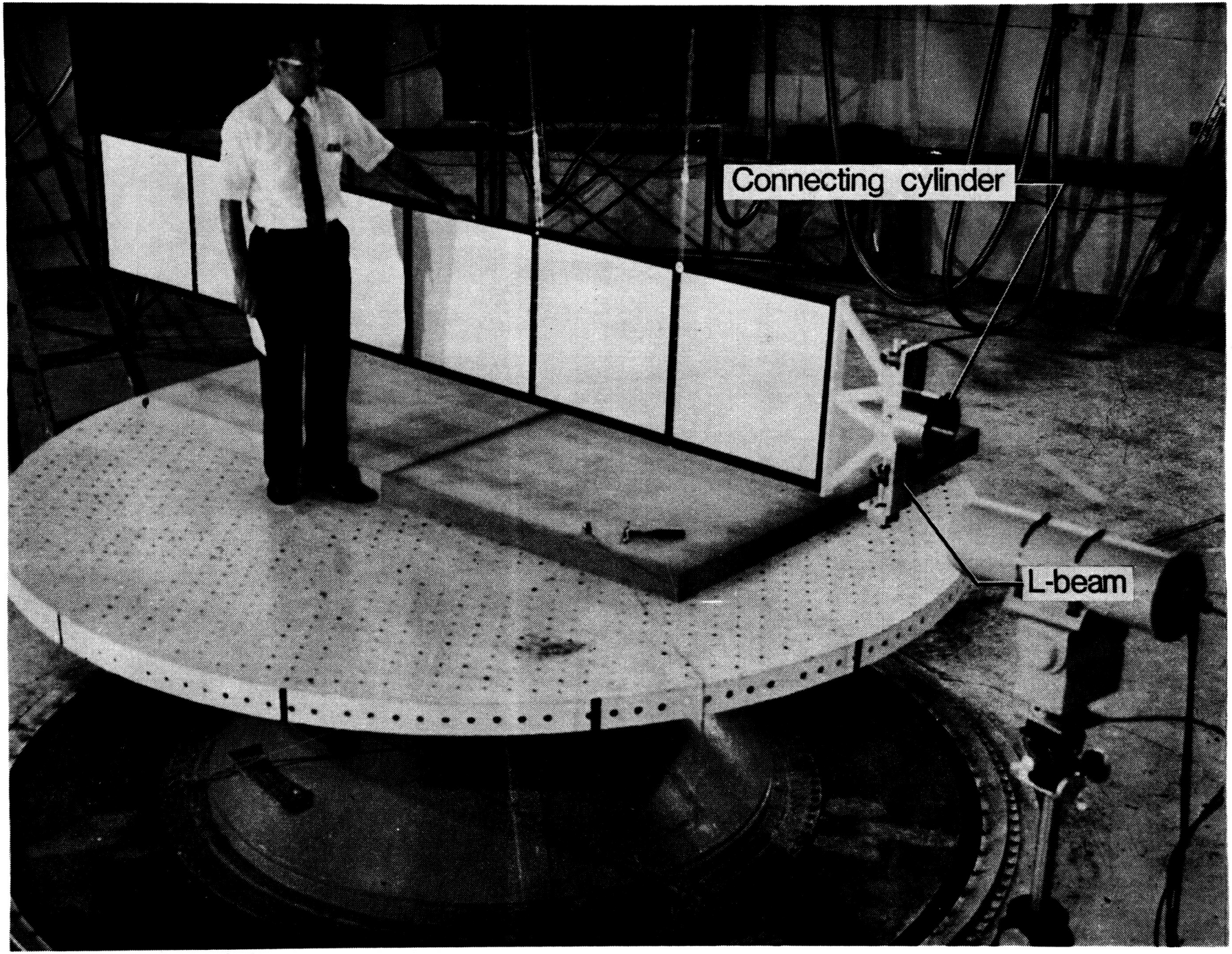

Figure 13. Completed Six Bay Solar Array Panel

ORIGINAL PAGE IS
OF POOR QUALITY

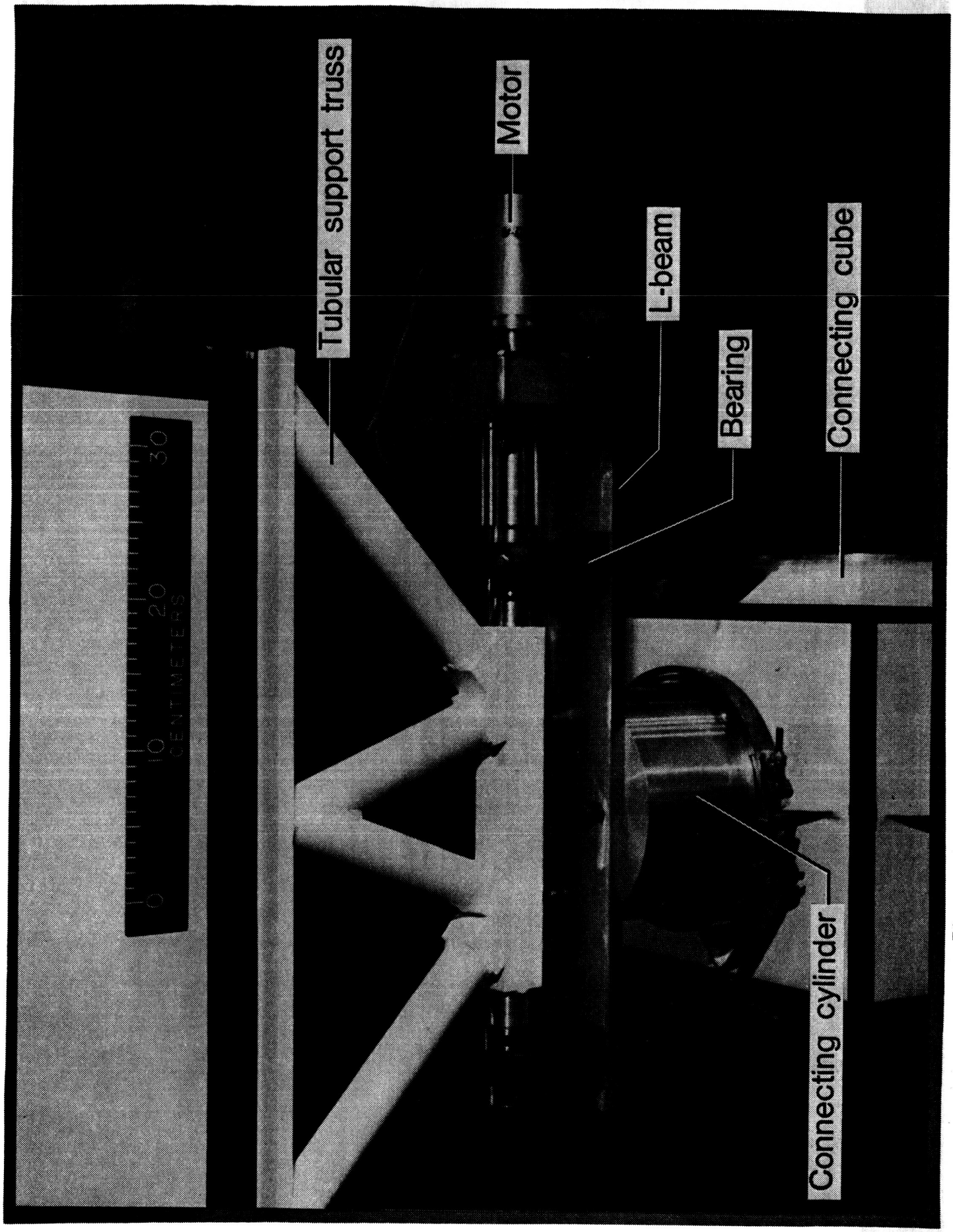

Figure 14. Solar Array Attachment Assembly

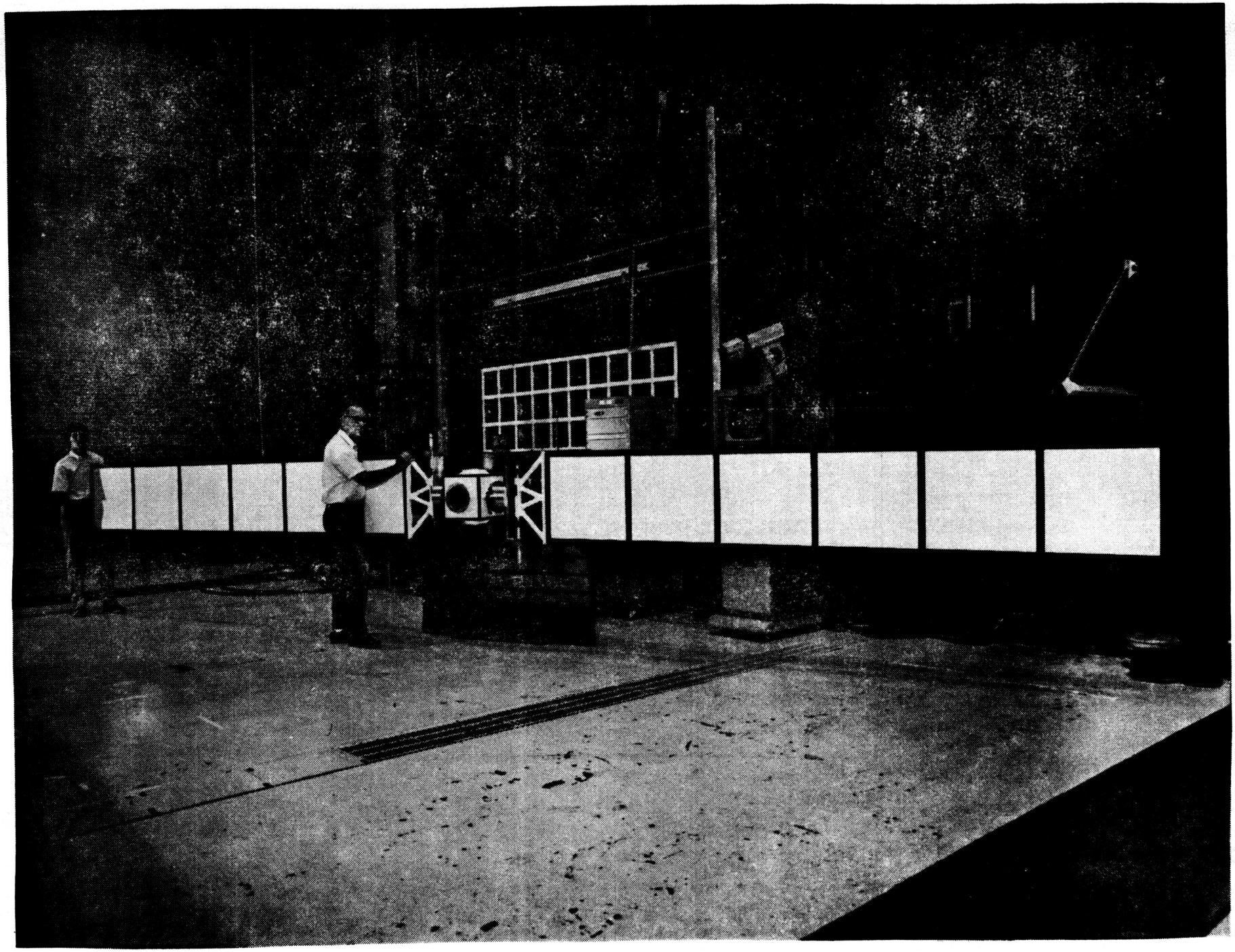

Figure 15. Solar Array Panels and Connecting Cube; Locked at 90 Degrees

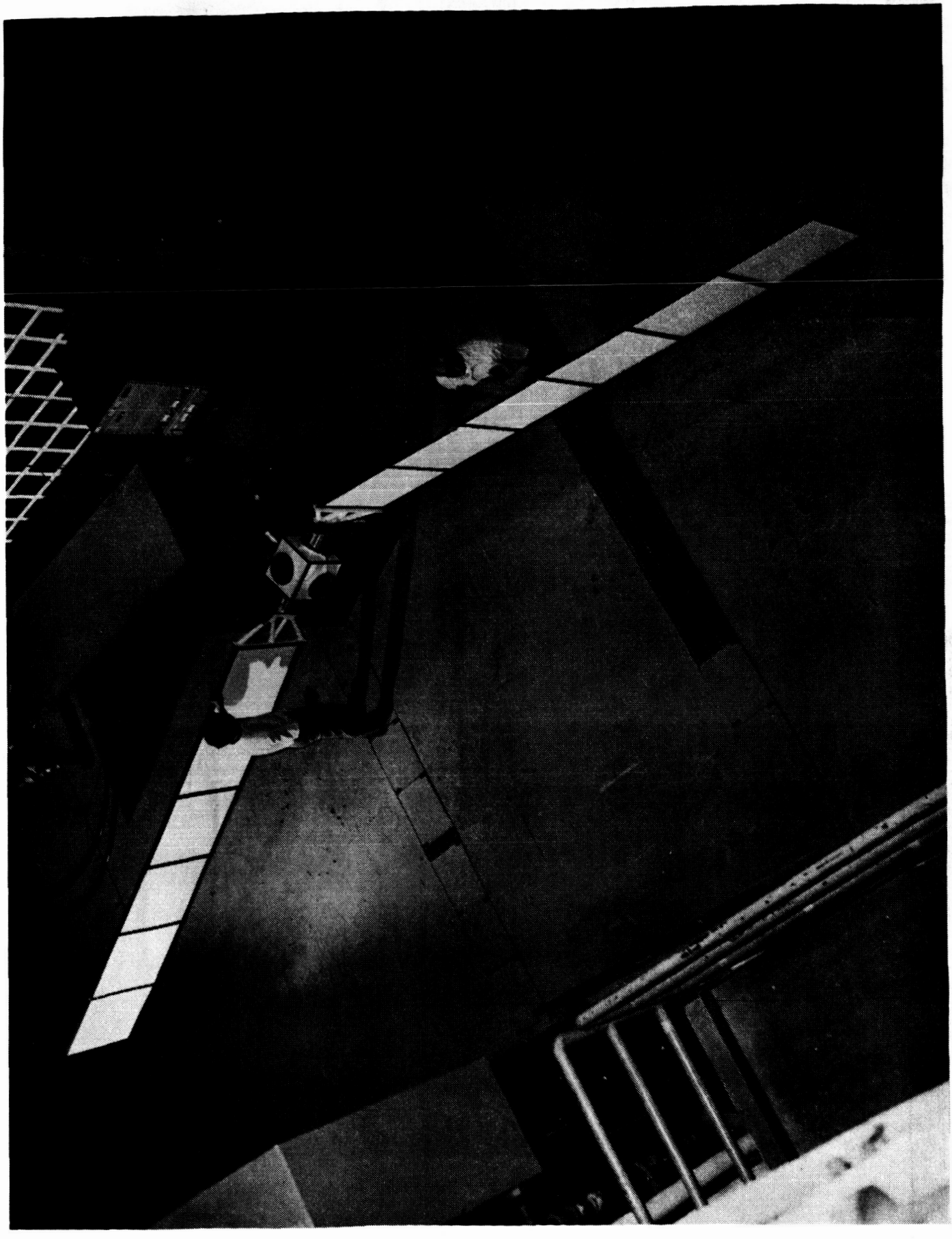

Figure 16. Solar Array Panels and Connecting Cube; Rotated

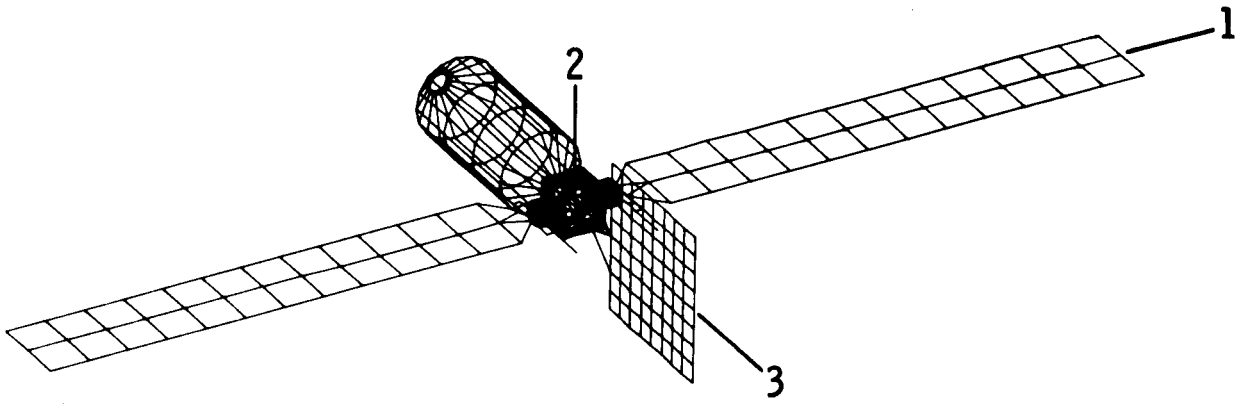

Figure 17. Analytical Model of the Generic Dynamic Model Without Cables

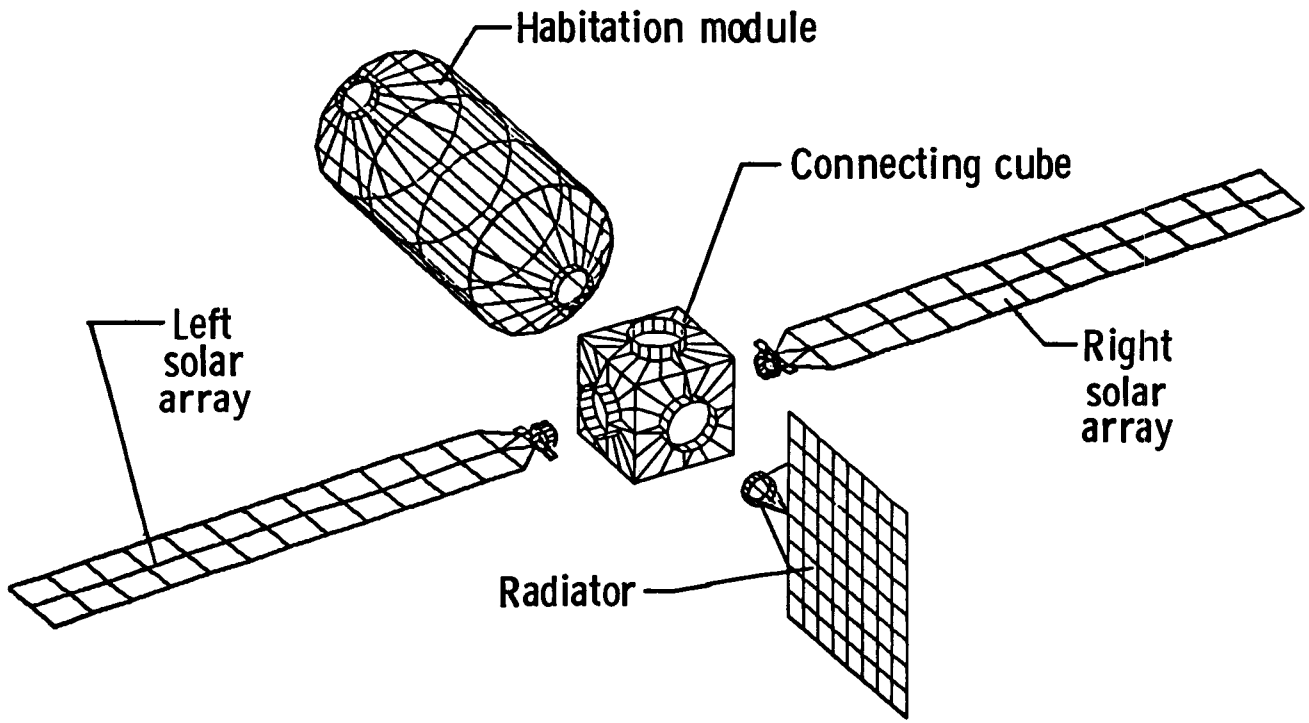

Figure 18. Analytical Substructure Models

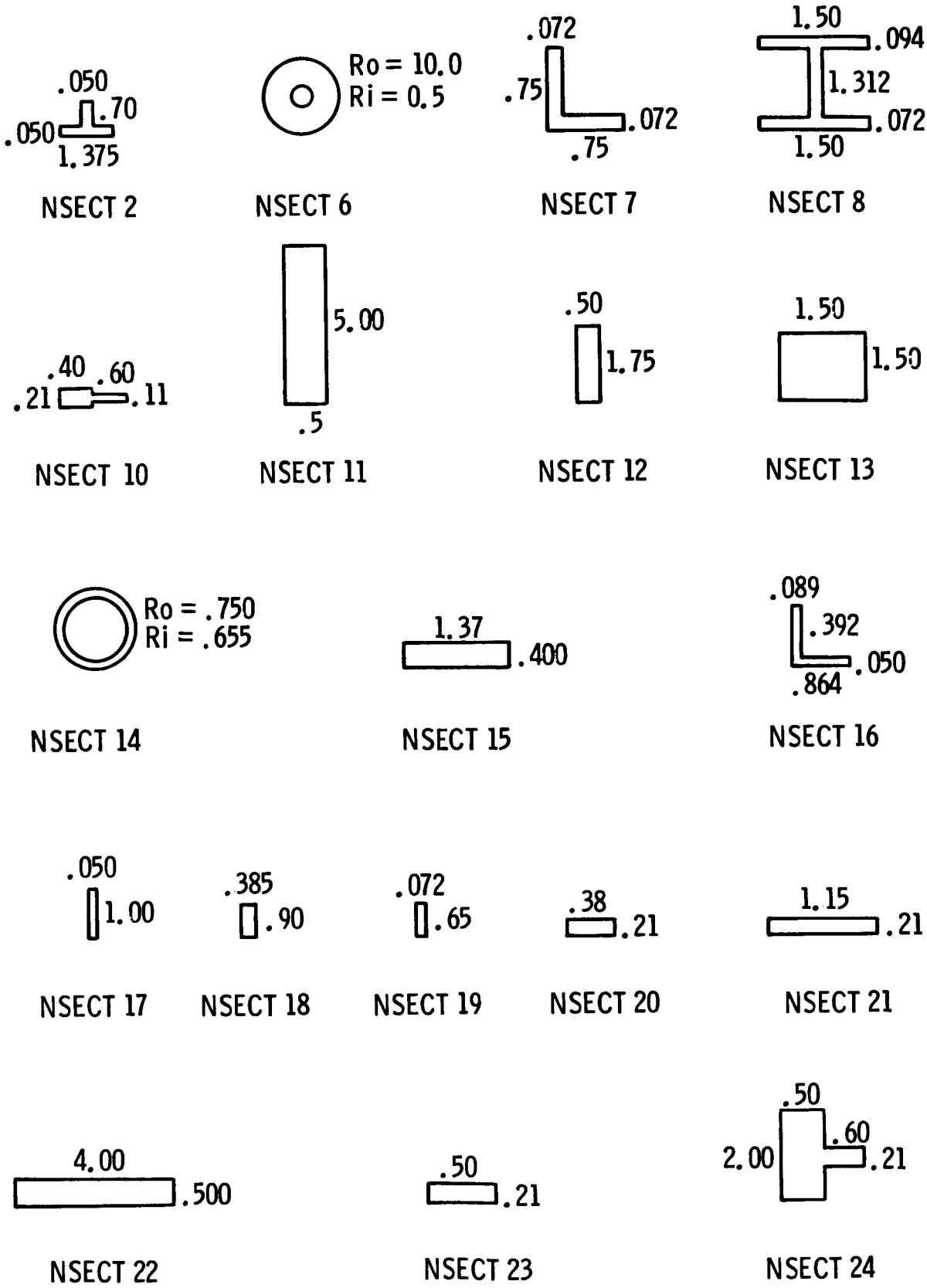

Figure 19. NSECT Section Properties

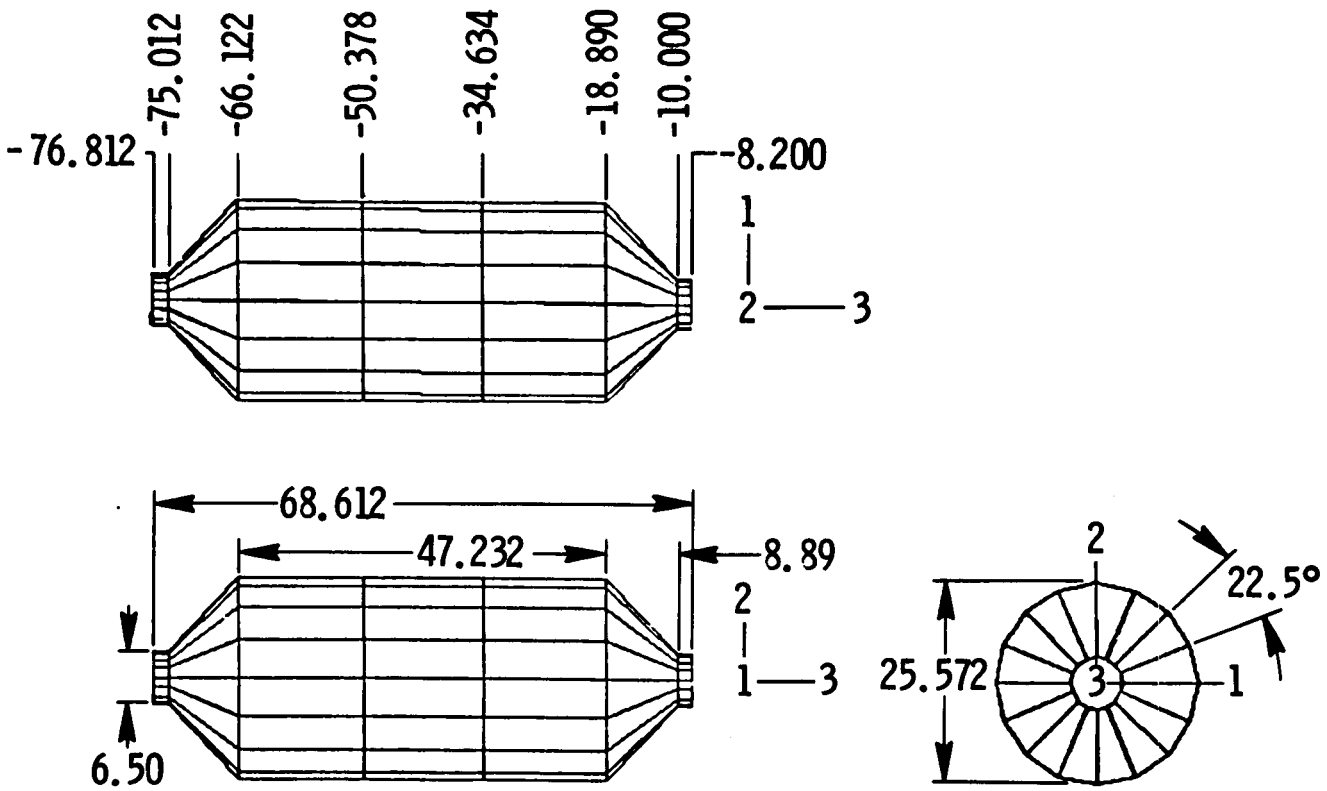

Figure 20. Analytical Habitation Module

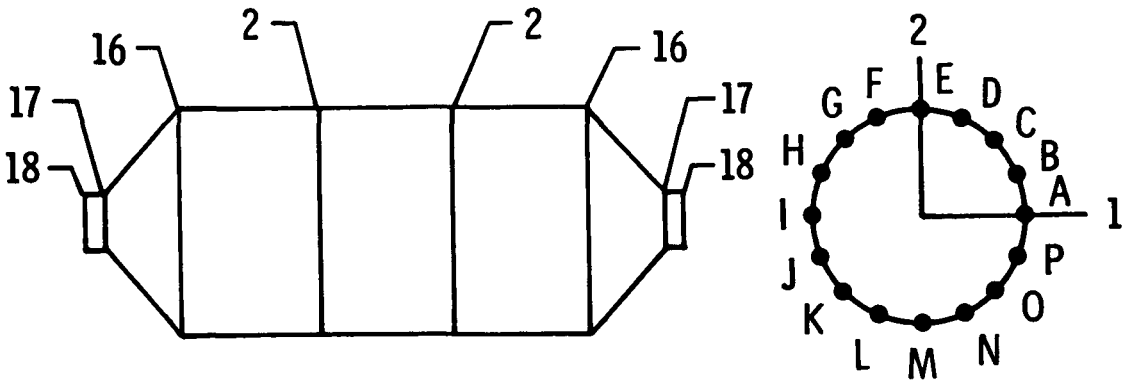

Station	A	B	C	D	E	F	G	H	I	J	K	L	M	N	O	P
	Connecting Grid Point Numbers															
16 rectangular ring elements NSECT = 18																
-76.812	33	34	35	36	37	38	39	40	41	42	43	44	45	46	47	48
16 rectangular ring elements NSECT = 17																
-75.012	49	50	51	52	53	54	55	56	57	58	59	60	61	62	63	64
16 angle ring elements NSECT = 16																
-66.122	65	66	67	68	69	70	71	72	73	74	75	76	77	78	79	80
32 tee ring elements NSECT = 2																
-50.378	81	82	83	84	85	86	87	88	89	90	91	92	93	94	95	96
-34.634	97	98	99	100	101	102	103	104	105	106	107	108	109	110	111	112
16 angle ring elements NSECT = 16																
-18.890	113	114	115	116	117	118	119	120	121	122	123	124	125	126	127	128
16 rectangular ring elements NSECT = 17																
-10.000	129	130	131	132	133	134	135	136	137	138	139	140	141	142	143	144
16 rectangular ring elements NSECT = 18																
-8.200	145	146	147	148	149	150	151	152	153	154	155	156	157	158	159	160

Figure 21. Habitation Module Grid Point and Ring Locations

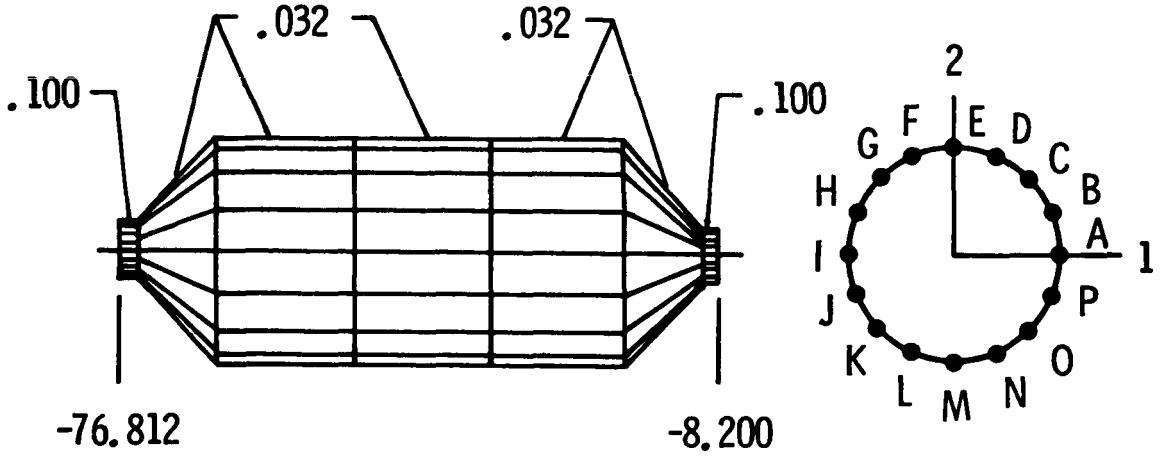

Station	A	B	C	D	E	F	G	H	I	J	K	L	M	N	O	P
	Connecting Grid Point Numbers															
16 plate elements 0.100-in. thick																
-76.812	33	34	35	36	37	38	39	40	41	42	43	44	45	46	47	48
-75.012	49	50	51	52	53	54	55	56	57	58	59	60	61	62	63	64
80 plate elements 0.032-in. thick																
-75.012	49	50	51	52	53	54	55	56	57	58	59	60	61	62	63	64
-66.122	65	66	67	68	69	70	71	72	73	74	75	76	77	78	79	80
-50.378	81	82	83	84	85	86	87	88	89	90	91	92	93	94	95	96
-34.634	97	98	99	100	101	102	103	104	105	106	107	108	109	110	111	112
-18.890	113	114	115	116	117	118	119	120	121	122	123	124	125	126	127	128
-10.000	129	130	131	132	133	134	135	136	137	138	139	140	141	142	143	144
16 plate elements 0.100-in. thick																
-10.000	129	130	131	132	133	134	135	136	137	138	139	140	141	142	143	144
-8.200	145	146	147	148	149	150	151	152	153	154	155	156	157	158	159	160

Figure 22. Habitation Module Plate Elements

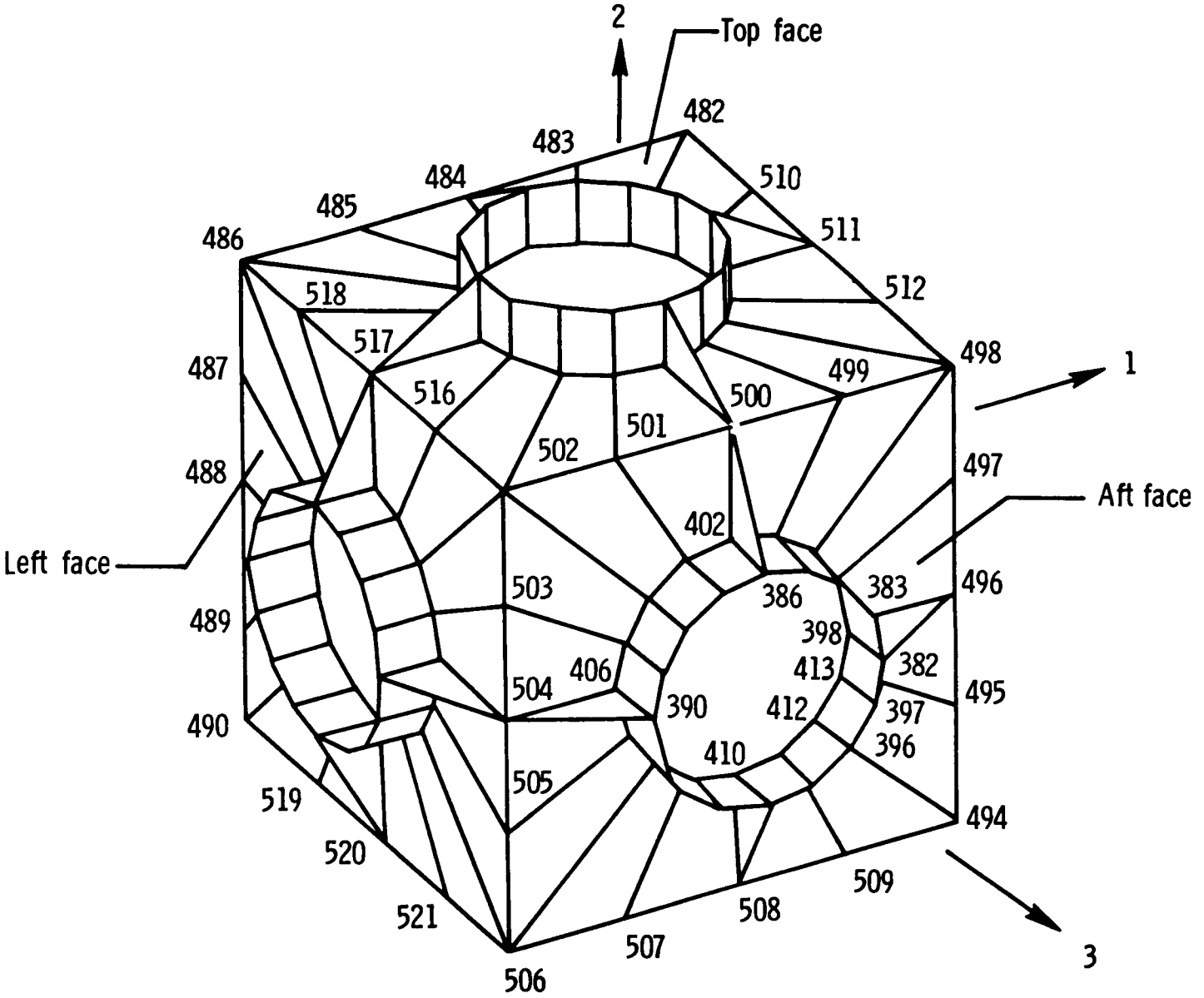

Figure 23. Connecting Cube Analytical Model

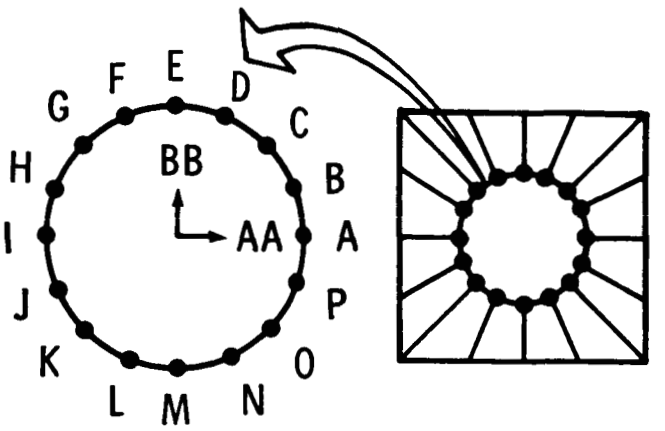

Face(AA,BB)*	A	B	C	D	E	F	G	H	I	J	K	L	M	N	O	P
	Connecting Grid Point Numbers															
96 rectangular ring elements NSECT = 18 clamp ring																
Forward(-1,2)	153	152	151	150	149	148	147	146	145	160	159	158	157	156	155	154
Aft(1,2)	382	383	384	385	386	387	388	389	390	391	392	393	394	395	396	397
Right(-3,2)	214	213	212	211	210	209	298	207	206	221	220	219	218	217	216	215
Left((3,2)	267	268	269	270	271	272	273	274	275	276	277	278	279	280	281	282
Top(1,-3)	414	415	416	417	418	419	420	421	422	423	424	425	426	427	428	429
Bottom(-1,-3)	454	455	456	457	458	459	460	461	446	447	448	449	450	451	452	453
96 rectangular ring elements NSECT = 19 cylinder face intersection																
Forward(-1,2)	169	168	167	166	165	164	163	162	161	176	175	174	173	172	171	170
Aft(1,2)	398	399	400	401	402	403	404	405	406	407	408	409	410	411	412	413
Right(-3,2)	222	223	224	225	226	227	228	229	230	231	232	233	234	235	236	237
Left(3,2)	283	284	285	286	287	288	289	290	291	292	293	294	295	296	297	298
Top(1,-3)	430	431	432	433	434	435	436	437	438	439	440	441	442	443	444	445
Bottom(-1,-3)	470	471	472	473	474	475	476	477	462	463	464	465	466	467	468	469

* See Figure 23 for coordinate directions (AA,BB)

Figure 24. Connecting Cube Ring Beam Elements

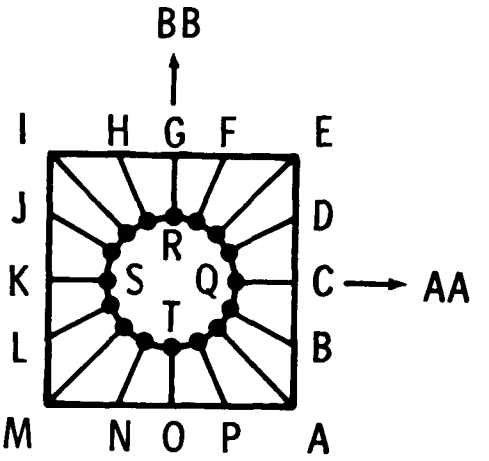

	A	B	C	D	E	F	G	H	I	J	K	L	M	N	O	P
Face(AA,BB)*	Connecting Grid Point Numbers															
48 angle beam elements NSECT = 7 edge																
Forward(-1,2)	490	489	488	487	486	485	484	483	482	481	480	479	478	493	492	491
Aft(1,2)	494	495	496	497	498	499	500	501	502	503	504	505	506	507	508	509
Right(-3,2)	478	479	480	481	482	510	511	512	498	497	496	495	494	513	514	515
Left(3,2)	506	505	504	503	502	516	517	518	486	487	488	489	490	519	520	521
Top(1,-3)	498	512	511	510	482	483	484	485	486	518	517	516	502	501	500	499
Bottom(-1,-3)	506	521	520	519	490	491	492	493	478	515	514	513	494	509	508	507

	C	Q	G	R	K	S	O	T
24 I shaped beam elements NSECT = 8 bending stiffeners								
Forward(-1,2)	488	169	484	165	480	161	492	173
Aft(1,2)	496	398	500	402	504	406	508	410
Right(-3,2)	480	222	511	226	496	230	514	234
Left(3,2)	504	283	517	287	488	291	520	295
Top(1,-3)	511	430	484	434	517	438	500	442
Bottom(-1,-3)	520	470	492	474	514	462	508	466

* See Figure 23 for coordinate directions (AA,BB)

Figure 25. Connecting Cube Edge and Stiffener Beam Elements

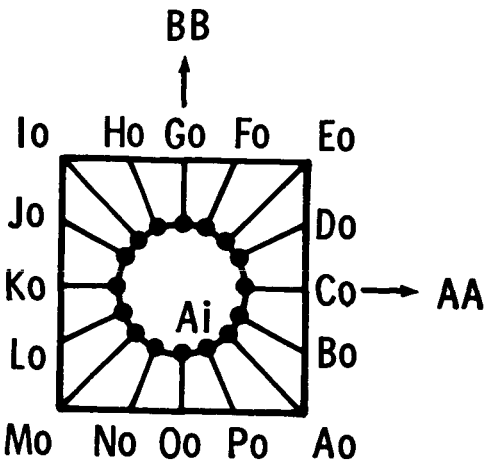

	Ai	Bi	Ci	Di	Ei	Fi	Gi	Hi	Ii	Ji	Ki	Li	Mi	Ni	Oi	Pi
	Ao	Bo	Co	Do	Eo	Fo	Go	Ho	Io	Jo	Ko	Lo	Mo	No	Oo	Po
Face(AA,BB)*	Connecting Grid Point Numbers															
96 plate elements 0.064 in. thick																
Forward(-1,2)	171	170	169	168	167	166	165	164	163	162	161	176	175	174	173	172
	490	489	488	487	486	485	484	483	482	481	480	479	478	493	492	491
Aft(1,2)	412	413	398	399	400	401	402	403	404	405	406	407	308	409	410	411
	494	495	496	497	498	499	500	501	502	503	504	505	506	507	508	509
Right(-3,2)	236	237	222	223	224	225	226	227	228	229	230	231	232	233	234	235
	478	479	480	481	482	510	511	512	498	497	496	495	494	513	514	515
Left(3,2)	297	298	283	284	285	286	287	288	289	290	291	292	293	294	295	296
	506	505	504	503	502	516	517	518	486	487	488	489	490	519	520	521
Top(1,-3)	444	445	430	431	432	433	434	435	436	437	438	439	440	441	442	443
	498	512	511	510	482	483	484	485	486	518	517	516	502	501	500	499
Bottom(-1,-3)	468	469	470	471	472	473	474	475	476	477	462	463	464	465	466	467
	506	521	520	519	490	491	492	493	478	515	514	513	494	509	508	507

* See Figure 23 for coordinate directions (AA,BB)

Figure 26. Connecting Cube Face Plate Elements

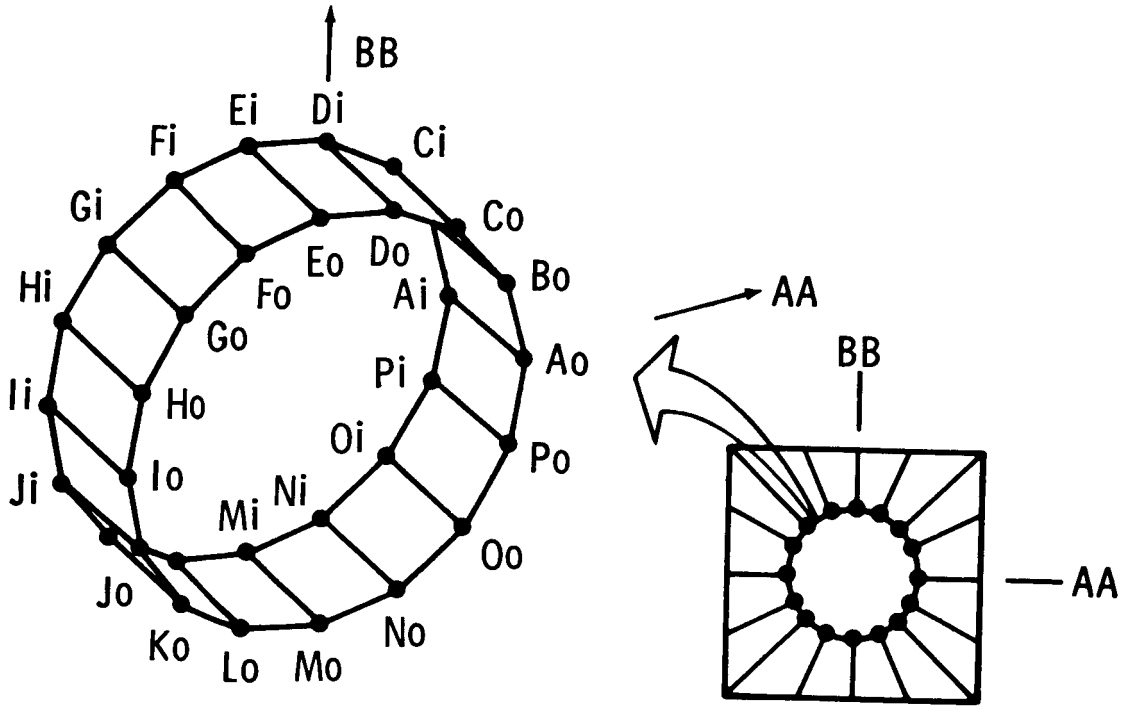

	Ao	Bo	Co	Do	Eo	Fo	Go	Ho	Io	Jo	Ko	Lo	Mo	No	Oo	Po
	Ai	Bi	Ci	Di	Ei	Fi	Gi	Hi	Ii	Ji	Ki	Li	Mi	Ni	Oi	Pi

Face(AA,BB)*	Connecting Grid Point Numbers															
96 plate elements 0.100 in. thick																
Forward(-1,2)	153	152	151	150	149	148	147	146	145	160	159	158	157	156	155	154
	169	168	167	166	165	164	163	162	161	176	175	174	173	172	171	170
Aft(1,2)	382	383	384	385	386	387	388	389	390	391	392	393	394	395	396	397
	398	399	400	401	402	403	404	405	406	407	408	409	410	411	412	413
Right(-3,2)	206	207	208	209	210	211	212	213	214	215	216	217	218	219	220	221
	222	223	224	225	226	227	228	229	230	231	232	233	234	235	236	237
Left(3,2)	267	268	269	270	271	272	273	274	275	276	277	278	279	280	281	282
	283	284	285	286	287	288	289	290	291	292	293	294	295	296	297	298
Top(1,-3)	414	415	416	417	418	419	420	421	422	423	424	425	426	427	428	429
	430	431	432	433	434	435	436	437	438	439	440	441	442	443	444	445
Bottom(-1,-3)	454	455	456	457	458	459	460	461	446	447	448	449	450	451	452	453
	470	471	472	473	474	475	476	477	462	463	464	465	466	467	468	469

* See Figure 23 for coordinate directions (AA,BB)

Figure 27. Connecting Cube Attachment Cylinder Plate Elements

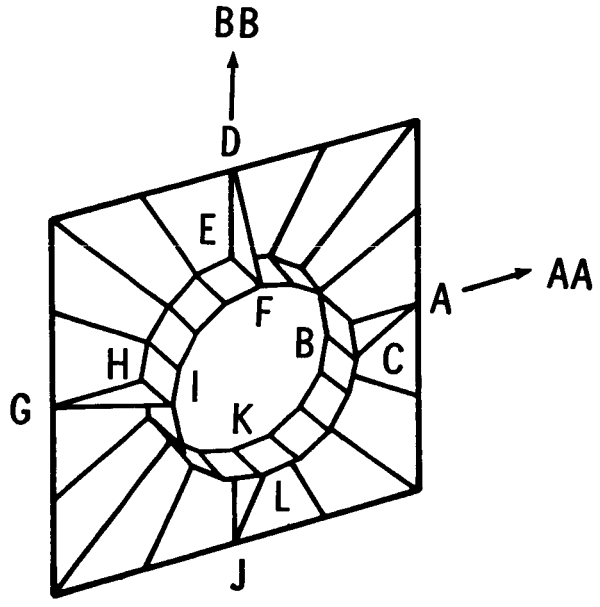

	A	B	C	D	E	F	G	H	I	J	K	L
Face(AA,BB)*	Connecting Grid Point Numbers											
24 plate elements 0.125 in thick												
Forward(-1,2)	488	169	153	484	165	149	480	161	145	492	173	157
Aft(1,2)	496	398	382	500	402	386	504	406	390	508	410	394
Right(-3,2)	480	222	206	511	226	210	496	230	214	514	234	218
Left(3,2)	504	283	267	517	287	271	488	291	275	520	295	279
Top(1,-3)	511	430	414	484	434	418	517	438	422	500	442	426
Bottom(-1,-3)	520	470	454	492	474	458	514	462	446	508	466	450

* See Figure 23 for coordinate directions (AA,BB)

Figure 28. Connecting Cube Triangular Stiffeners

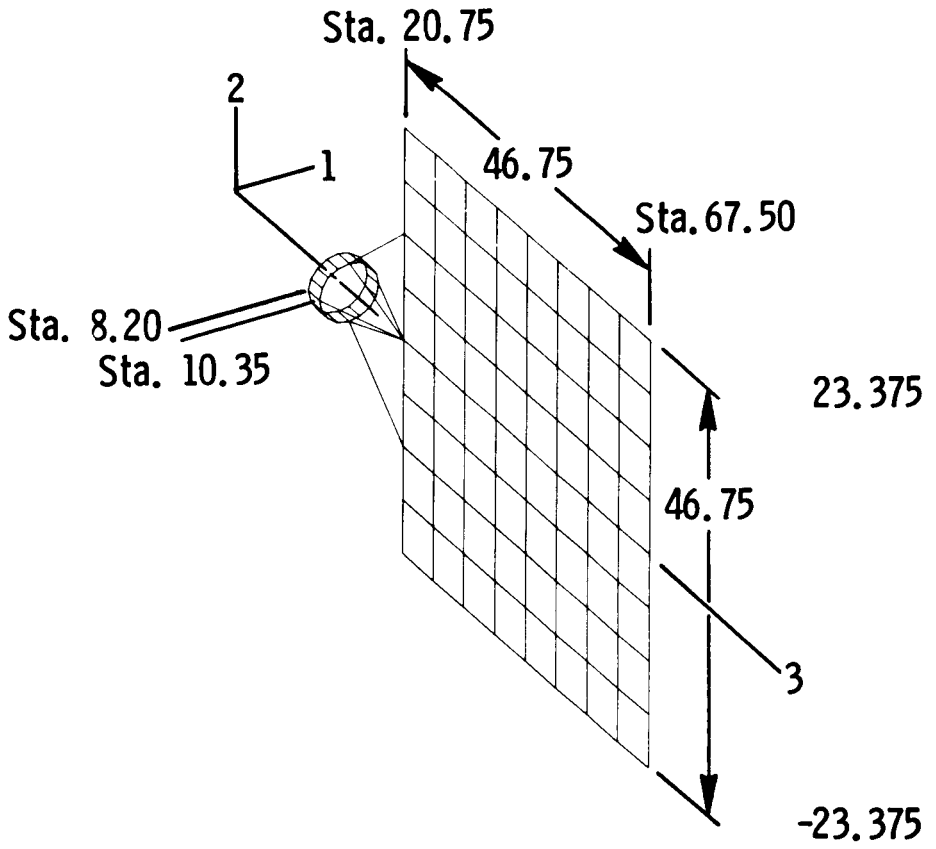

Figure 29. Radiator Analytical Model

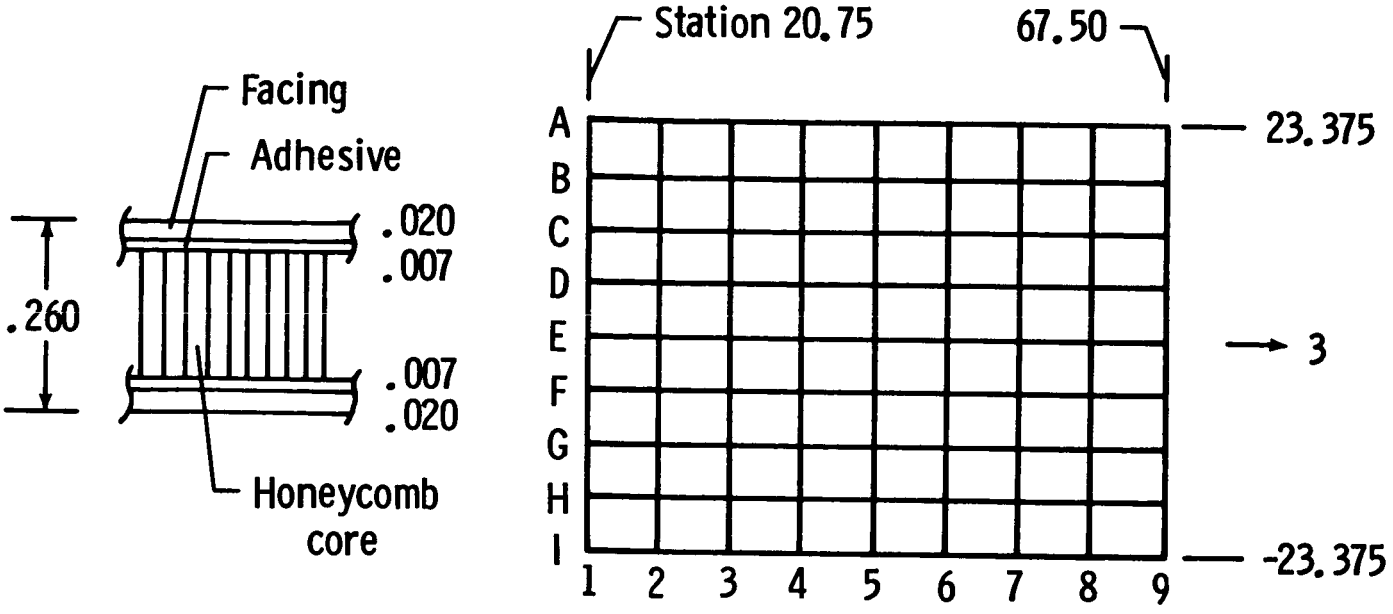

	Column								
	1	2	3	4	5	6	7	8	9
Row	Connecting Grid Point Numbers								
64 plate elements (5 layer laminate)									
A	379	370	361	352	343	334	325	316	307
B	378	369	360	351	342	333	324	315	306
C	377	368	359	350	341	332	323	314	305
D	376	367	358	349	340	331	322	313	304
E	375	366	357	348	339	330	321	312	303
F	374	365	356	347	338	329	320	311	302
G	373	364	355	346	337	328	319	310	301
H	372	363	354	345	336	327	318	309	300
I	371	362	353	344	335	326	317	308	299

Figure 30. Radiator Sandwich Honeycomb Plate Elements

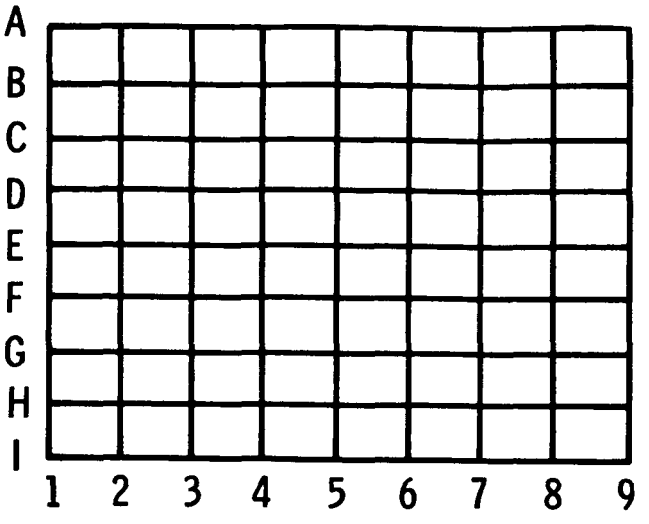

	1	2	3	4	5	6	7	8	9
Row	Connecting Grid Point Numbers								
24 rectangular edge beam elements, NSECT 23									
A	379	370	361	352	343	334	325	316	307
B									306
C									305
D									304
E									303
F									302
G									301
H									300
I	371	362	353	344	335	326	317	308	299

8 T base beam elements, NSECT 24	
A	379
B	378
C	377
D	376
E	375
F	374
G	373
H	372
I	371

Figure 31. Radiator Sandwich Edge and Base Beam Elements

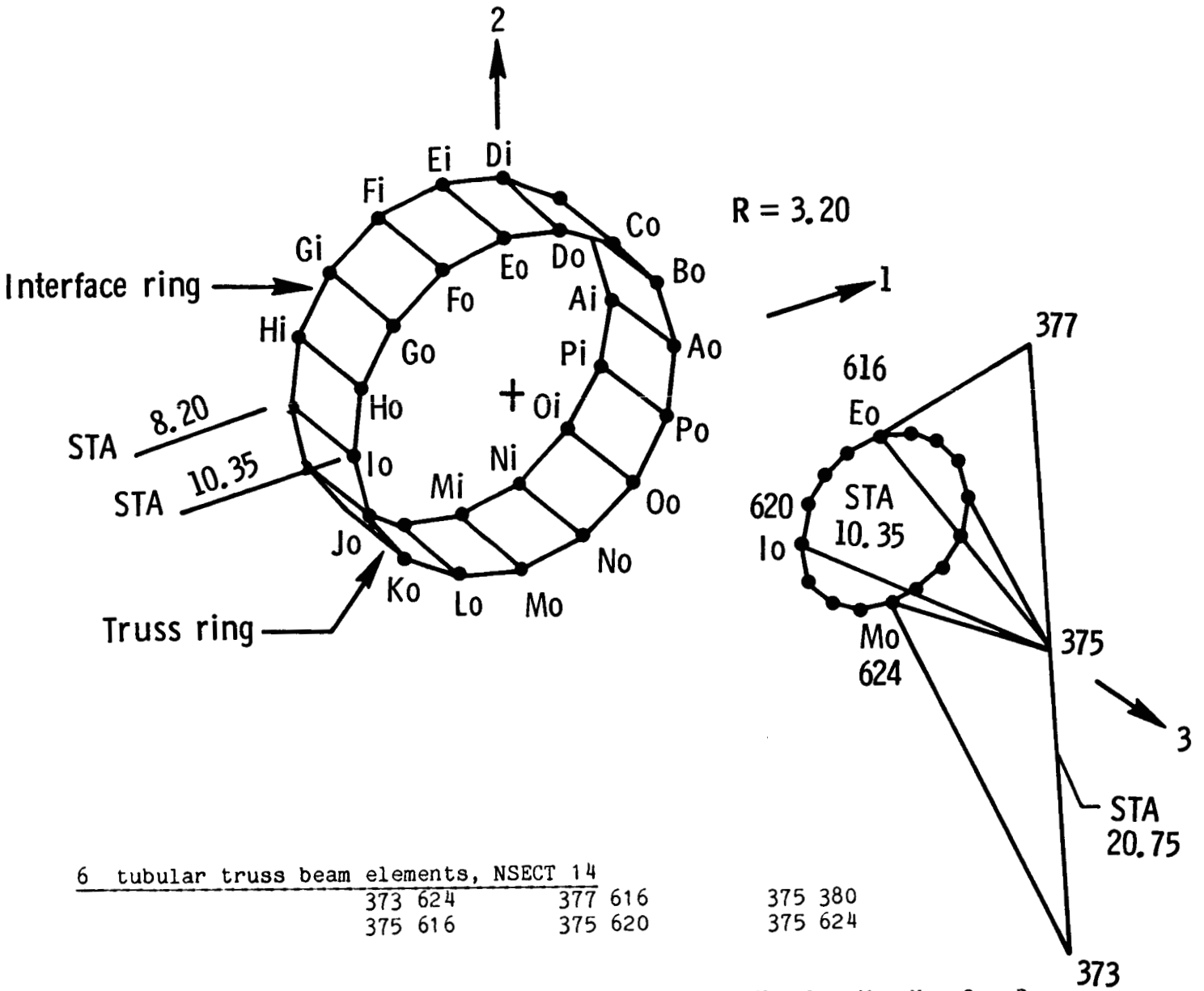

6 tubular truss beam elements, NSECT 14

373 624	377 616	375 380
375 616	375 620	375 624

A	B	C	D	E	F	G	H	I	J	K	L	M	N	O	P

Face	Connecting Grid Point Numbers

16 rectangular beam elements, NSECT 22, truss ring

380 381 614 615 616 617 618 619 620 621 622 623 624 625 626 627

16 rectangular beam elements, NSECT 18, interface ring

382 383 384 385 386 387 388 389 390 391 392 393 394 395 396 397

Ao	Bo	Co	Do	Eo	Fo	Go	Ho	Io	Jo	Ko	Lo	Mo	No	Oo	Po
Ai	Bi	Ci	Di	Ei	Fi	Gi	Hi	Ii	Ji	Ki	Li	Mi	Ni	Oi	Pi

16 plate elements 0.30 in. thick

380 381 614 615 616 617 618 619 620 621 622 623 624 625 626 627

382 383 384 385 386 387 388 389 390 391 392 393 394 395 396 397

Figure 32. Radiator Attachment Assembly Elements

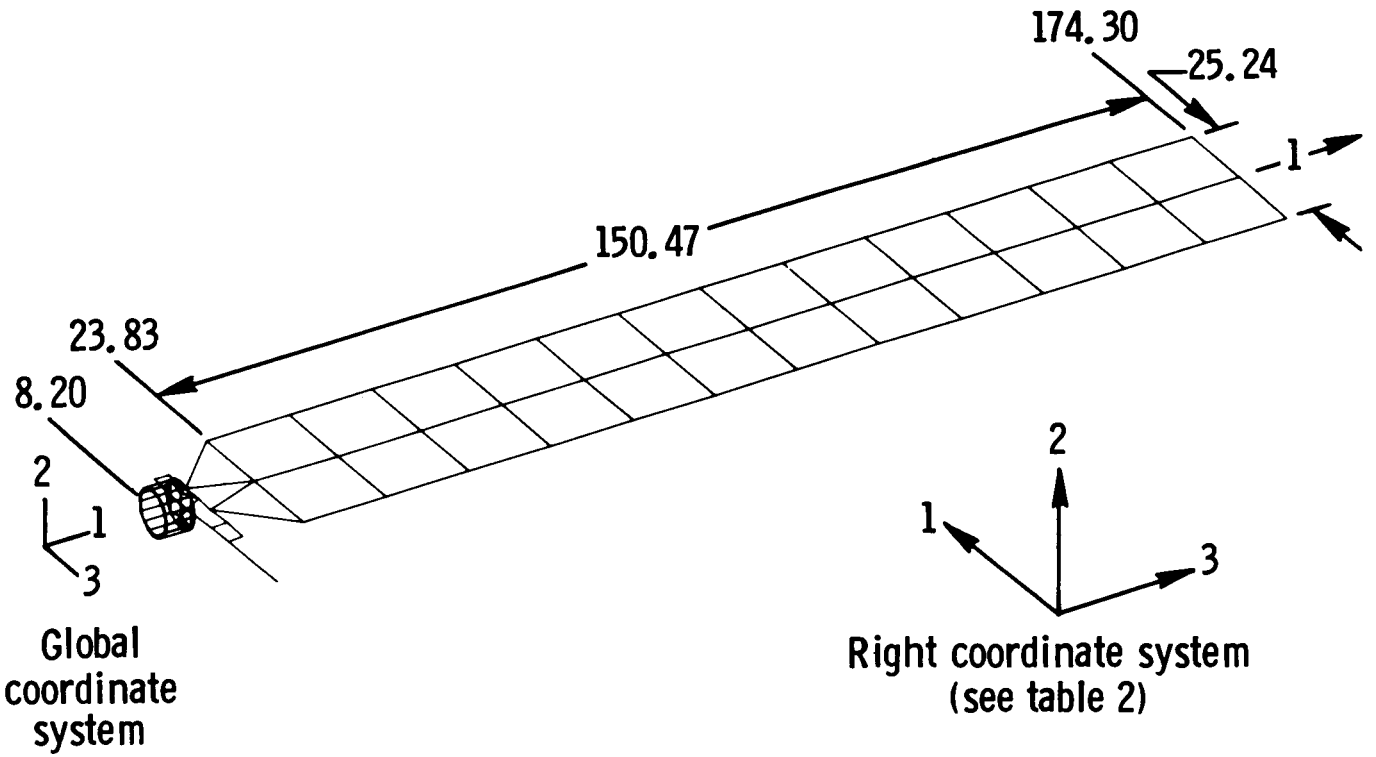

Figure 33. Right Solar Array Analytical Model

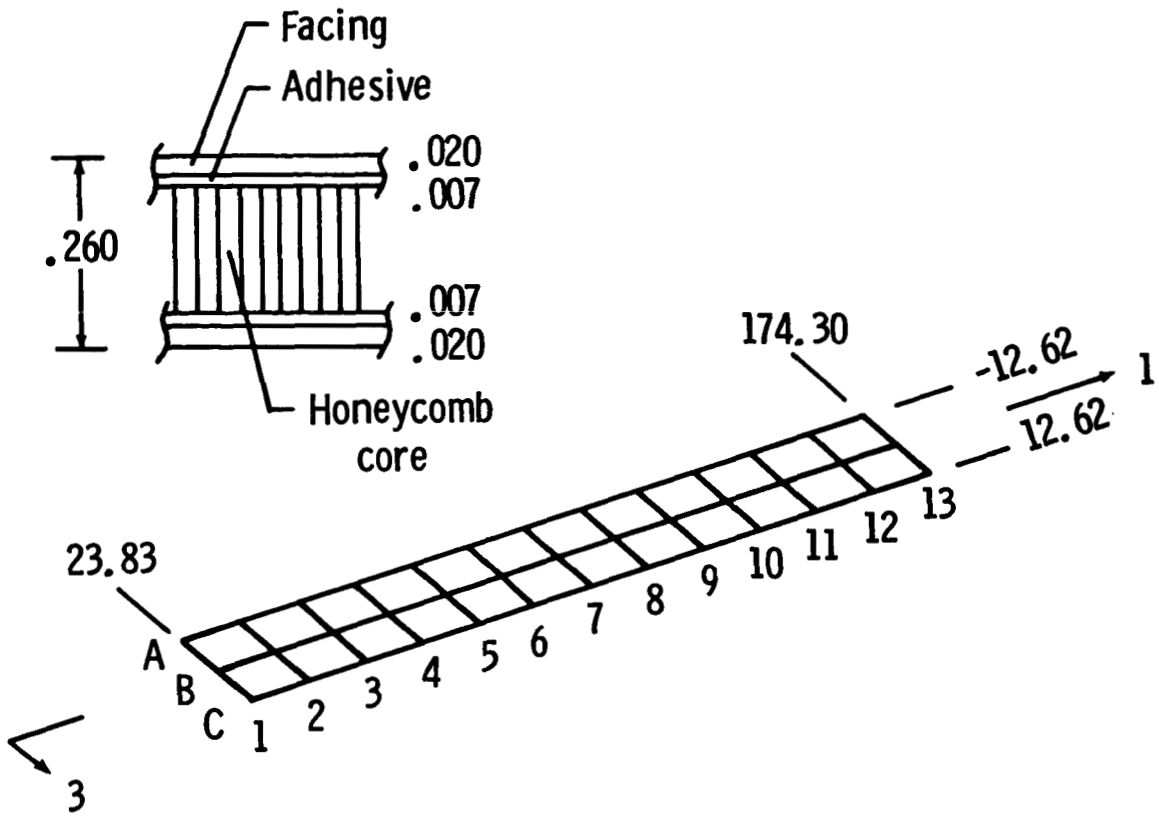

Row	Column												
	1	2	3	4	5	6	7	8	9	10	11	12	13
	Connecting Grid Point Numbers												
64 plate elements (5 layer laminate)													
A	203	200	197	194	191	188	185	182	179	639	636	633	630
B	202	199	196	193	190	187	184	181	178	638	635	632	629
C	201	198	195	192	189	186	183	180	177	637	634	631	628

Figure 34. Right Solar Array Sandwich Honeycomb Plate Elements

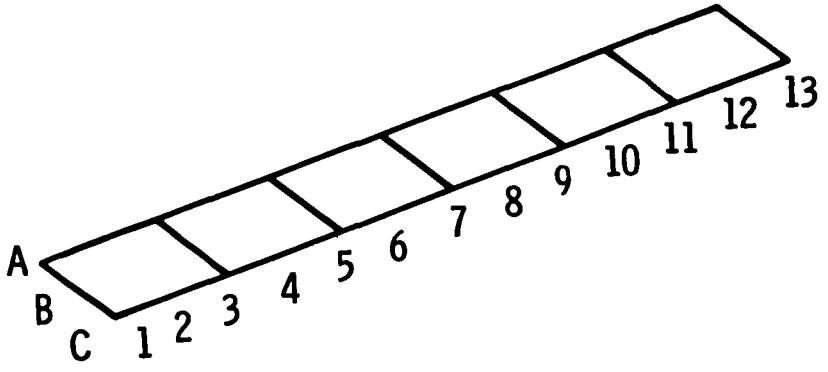

Column

	1	2	3	4	5	6	7	8	9	10	11	12	13
Row	Connecting Grid Point Numbers												
24 rectangular edge beam elements, NSECT 20													
A	203	200	197	194	191	188	185	182	179	639	636	633	630
B													
C	201	198	195	192	189	186	183	180	177	637	634	631	628

14 cross beam elements, 2 NSECT 24, 10 NSECT 21, 2 NSECT 10							
NSECT =	24	21	21	21	21	21	10
A	203	197	191	185	179	636	630
	|	|	|	|	|	|	|
B	202	196	190	184	178	635	629
	|	|	|	|	|	|	|
C	201	195	189	183	177	634	628

Figure 35. Right Solar Array Edge and Cross Beam Elements

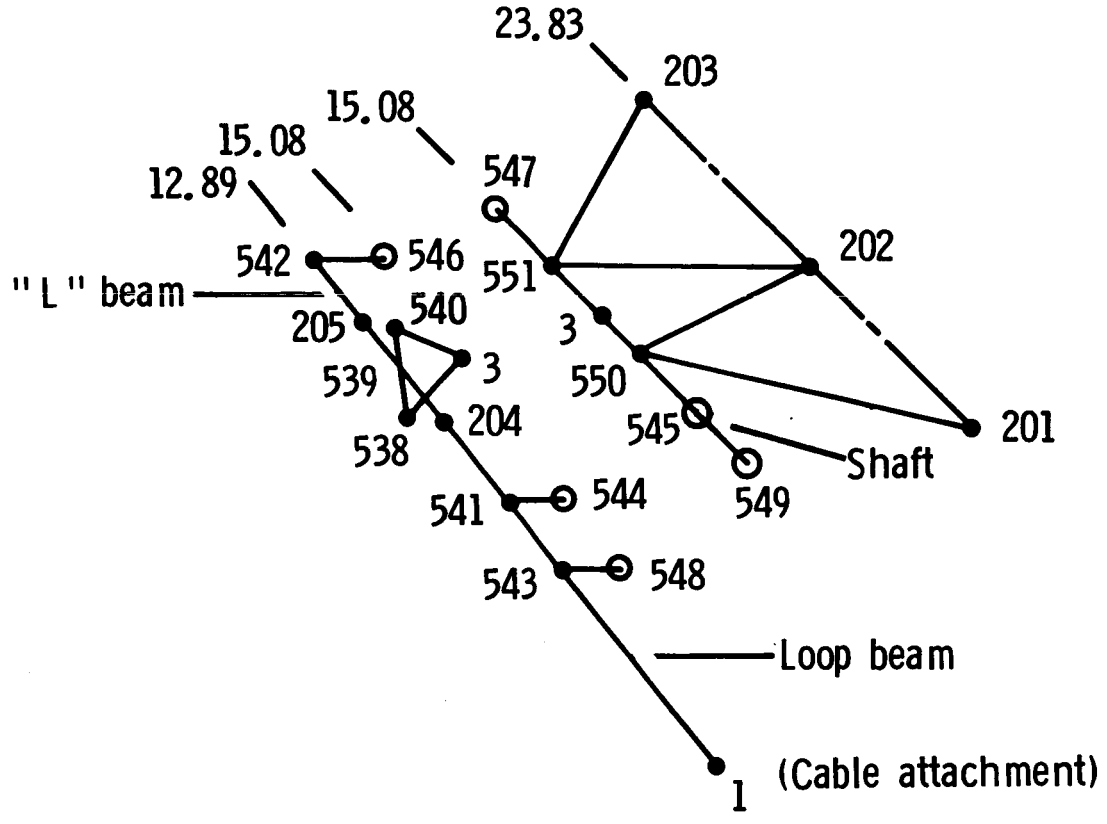

4 tubular truss beam elements, NSECT 14

201 550 202 550 202 551

203 551

5 square shaft beam elements, NSECT 13

549 545 550 3 551 547

6 rectangular L support beam elements and 2 bearing beam elements, NSECT 11

support beam	548 543 541 204 539 205 542
bearing beams	541 544 542 546

2 rectangular bulkhead attachment beams, NSECT 12

538 539 540

2 clamp stiffener beams, NSECT 6

3 538 3 540

Figure 36 Right Solar Array Truss, Shaft and L Support Beam

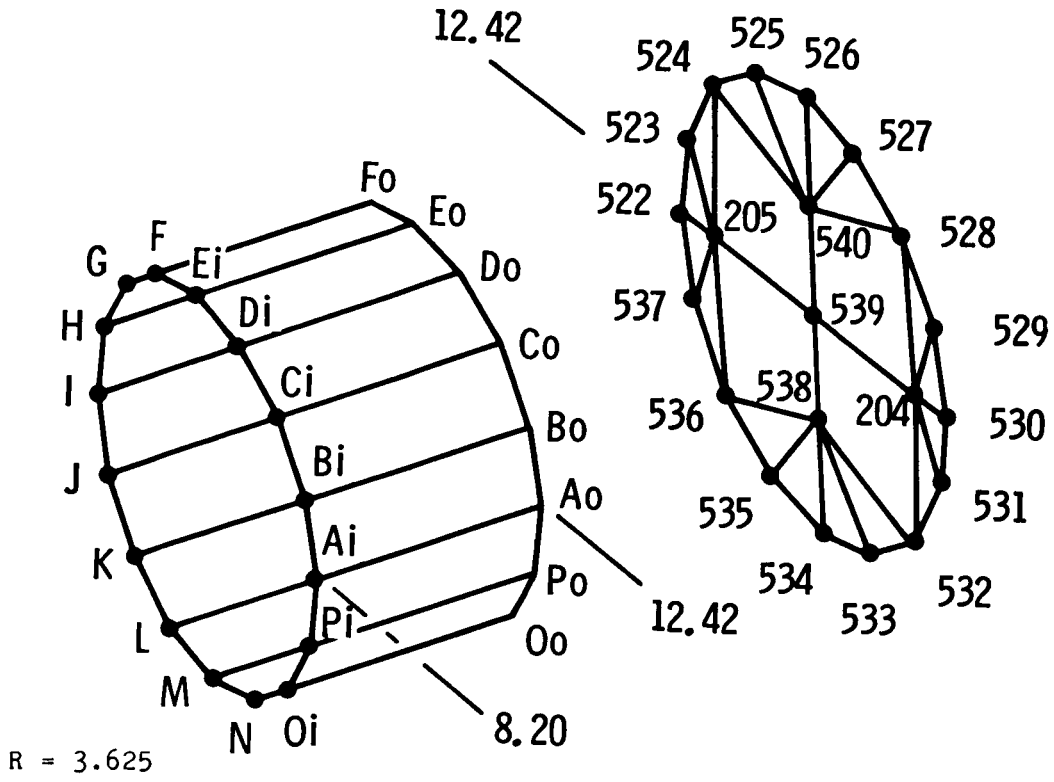

4 four node plate elements 0.440 in. thick

539	205	524	540
539	540	528	204
539	204	532	538
539	538	536	205

16 three node plate elements 0.440 in. thick

540	524	525	538	532	533
540	525	526	538	533	534
540	526	527	538	534	535
540	527	528	538	535	536
204	528	529	205	536	537
204	529	530	205	537	522
204	530	531	205	522	523
204	531	532	205	523	524

	A	B	C	D	E	F	G	H	I	J	K	L	M	N	O	P
from origin	Connecting Grid Point Numbers															

16 plate elements 0.150 in. thick

12.42	530	529	528	527	526	525	524	523	522	537	536	535	534	533	632	631
8.20	590	589	588	587	586	585	584	583	582	597	596	595	594	593	592	591

Figure 37. Right Solar Array Support Bulkhead and Cylinder Plate Elements

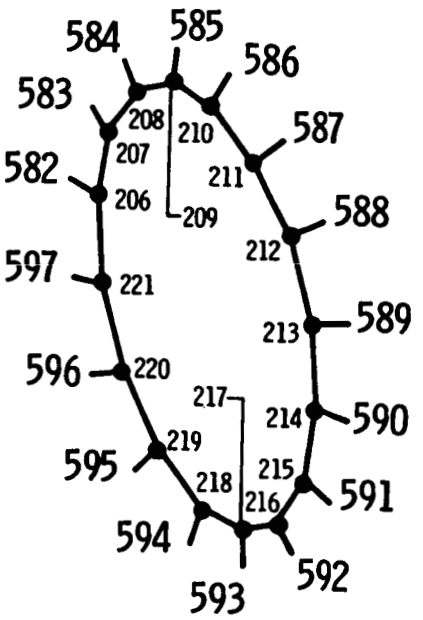

Ro = 3.625"
Ri = 3.25"
Station 8.20"

16 rectangular beam elements NSECT 18 circumferential

214 213 212 211 210 209 208 206 221 220 219 218 217 216 215

16 rectangular beam elements NSECT 15 radial

206 582	210 586	214 590	218 594
207 583	211 587	215 591	219 595
208 584	212 588	216 592	220 596
209 585	213 589	217 593	221 597

Figure 38. Right Solar Array Support Ring Beams

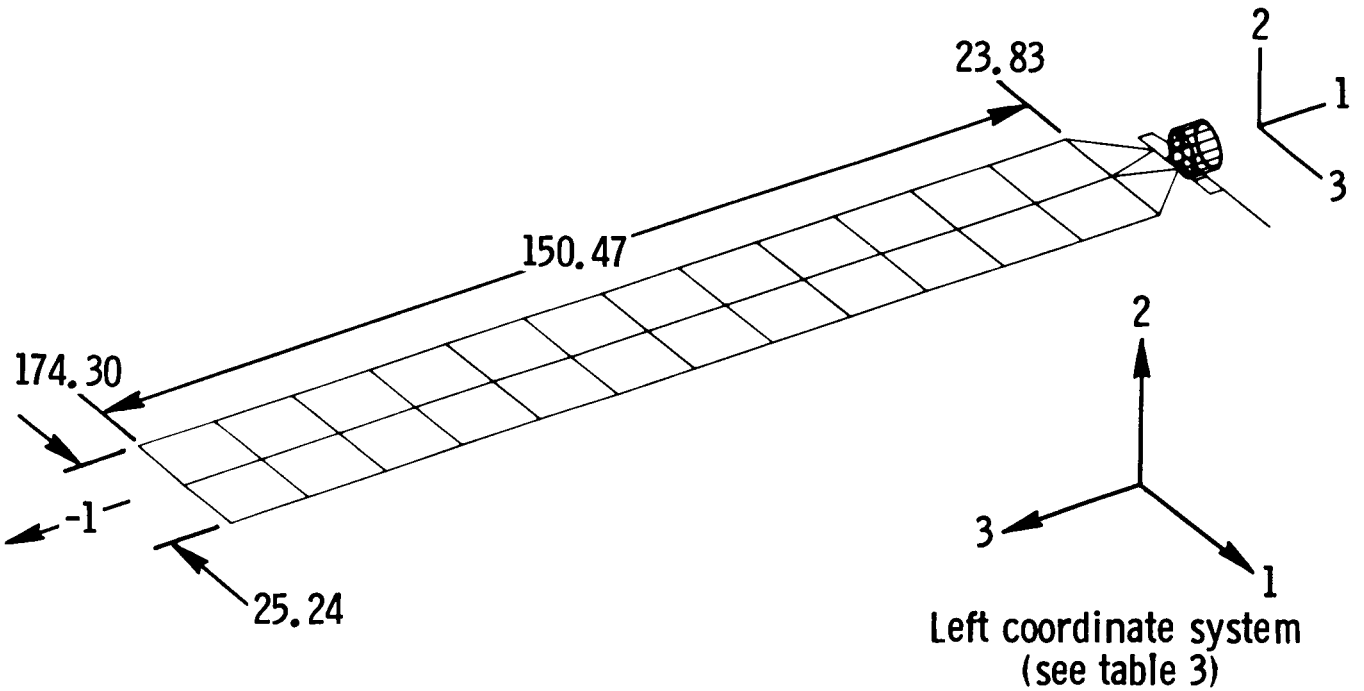

Figure 39. Left Solar Array Analytical Model

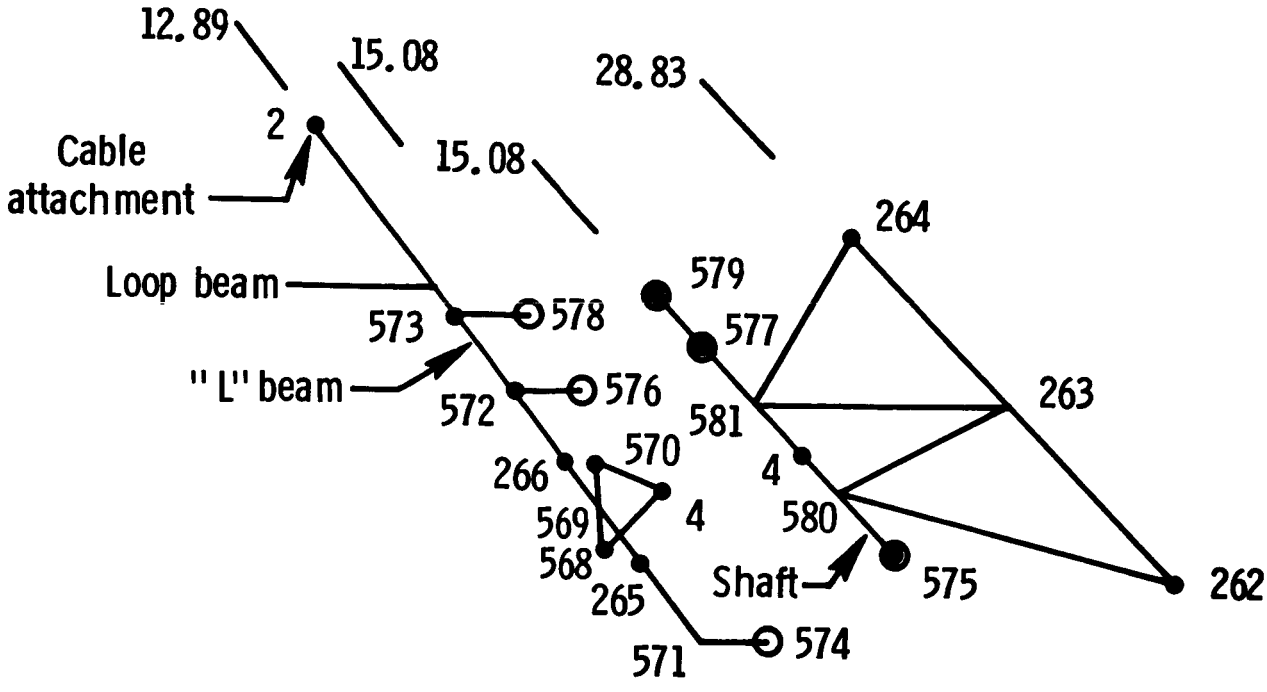

4 tubular truss beam elements, NSECT 14

262 580 263 580 263 581
264 581

5 square shaft beam elements, NSECT 13

575 580 4 581 577 579

6 rectangular L support beam elements, NSECT 11

571 265 569 266 572 573 578

2 rectangular bearing beam elements, NSECT 11

571 574 572 576

2 rectangular bulkhead attachment beams, NSECT 12

568 569 570

2 clamp stiffener beams, NSECT 6

4 568 4 570

Figure 40. Left Solar Array Truss, Shaft, and L Support Beams

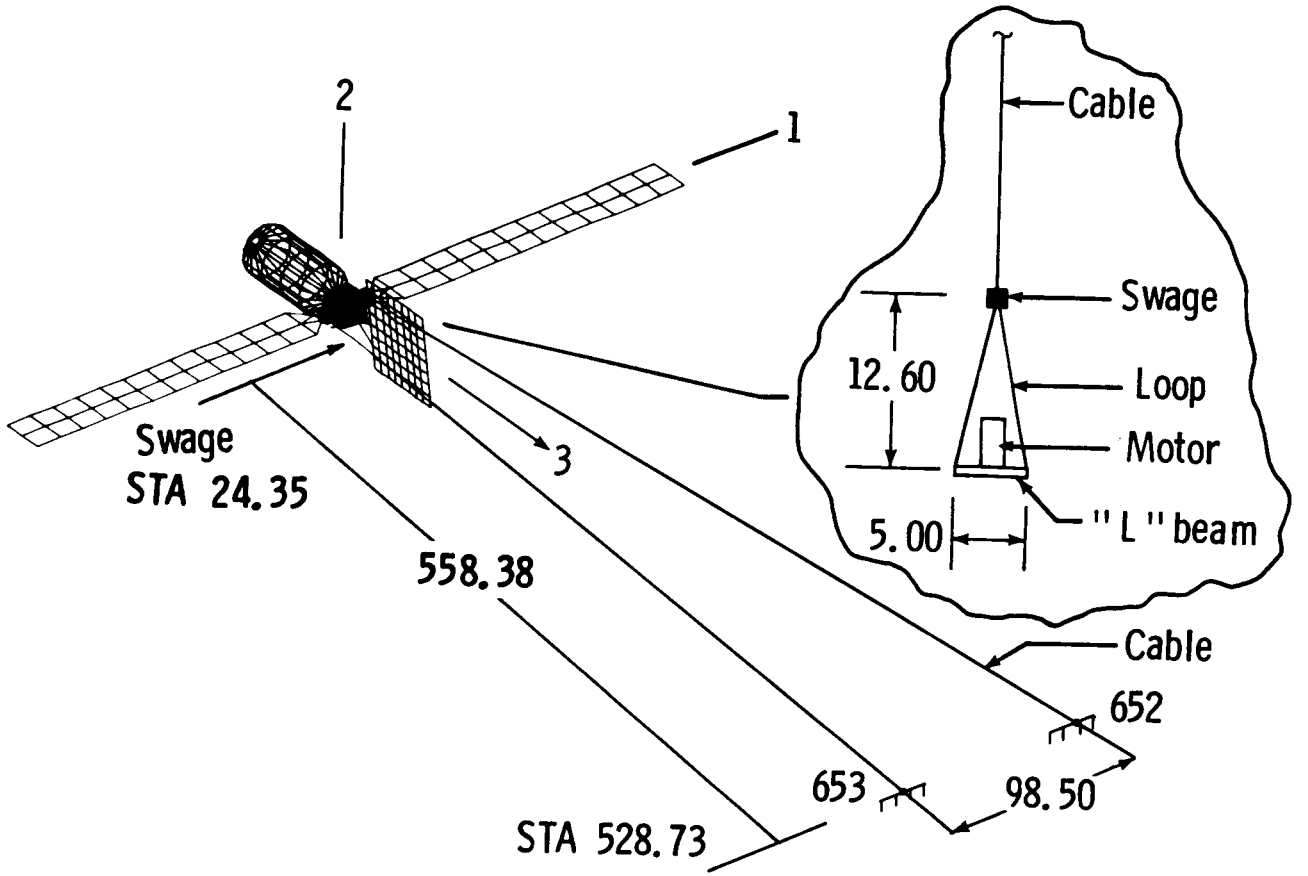

Figure 41. Analytical Model of the Generic Dynamic Model With Cables

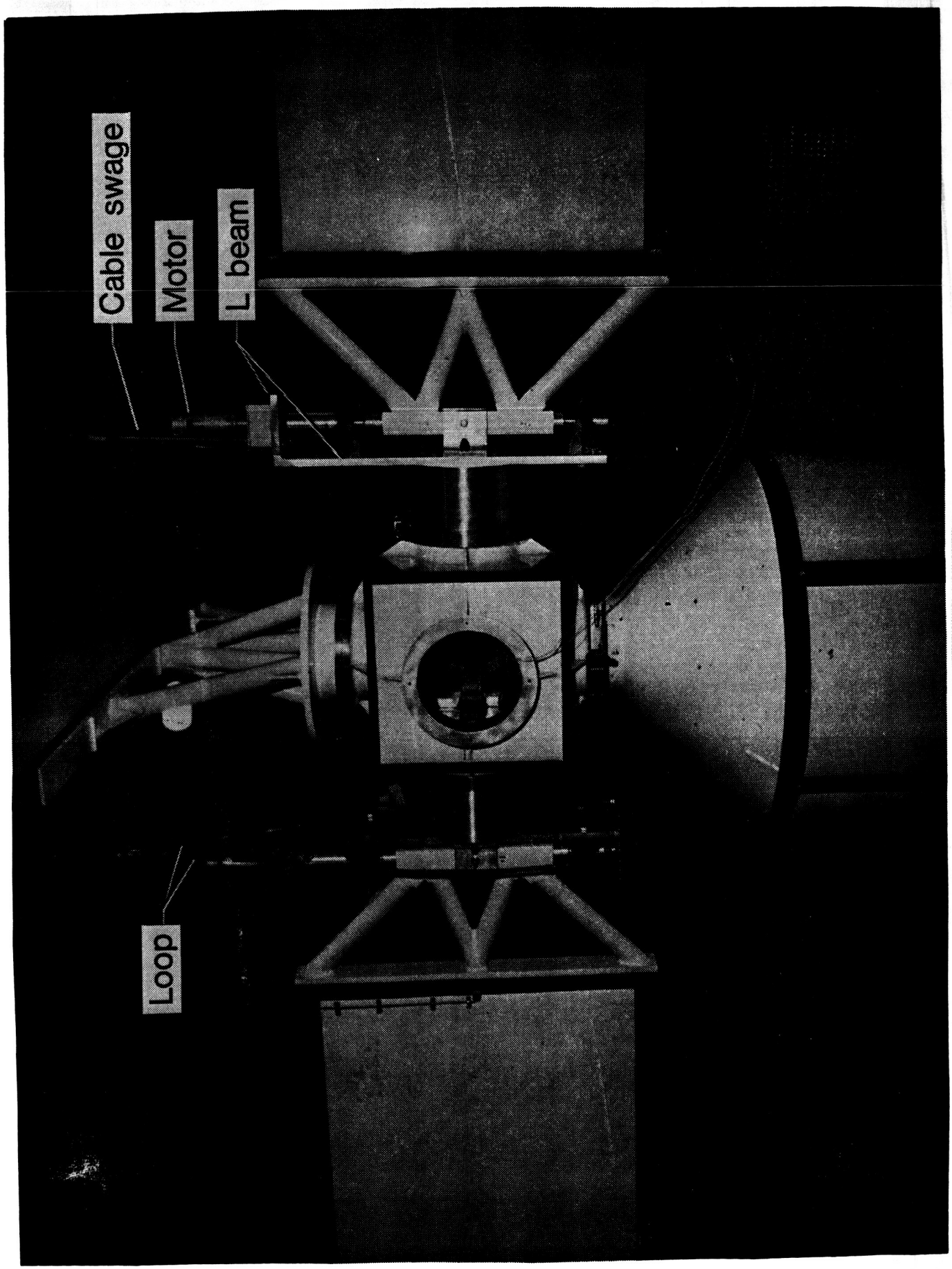

Figure 42. Detail Photograph of Cable Attachment

Standard Bibliographic Page

1. Report No.	2. Government Accession No.	3. Recipient's Catalog No.
NASA TM-87696		

4. Title and Subtitle	5. Report Date
Experimental and Analytical Generic Space Station Dynamic Models	MARCH 1986
	6. Performing Organization Code: 506-43-51-02
7. Author(s): W. Keith Belvin, Harold H. Edighoffer	8. Performing Organization Report No.
9. Performing Organization Name and Address: NASA Langley Research Center, Hampton, VA 23665	10. Work Unit No.
	11. Contract or Grant No.
12. Sponsoring Agency Name and Address: National Aeronautics and Space Administration, Washington, DC 20546	13. Type of Report and Period Covered: Technical Memorandum
	14. Sponsoring Agency Code

15. Supplementary Notes

16. Abstract

A dynamic model used for verification of analytical and experimental methods is documented. The model consists of five substructures to simulate the multi-body, low frequency nature of large space structures. Design considerations which led to a fundamental vibration frequency of less than one Hz are described. Finite element analysis used to predict the vibration modes and frequencies of the experimental model is presented. In addition, modeling of cable suspension effects using prestressed vibration analysis is described. Details of the experimental and analytical models are included to permit replication of the study. Results of the modal vibration tests and analysis are presented in a separate document.

17. Key Words (Suggested by Authors(s))	18. Distribution Statement
Ground Vibration Tests Modal Analysis Scaled Models Large Space Structures	Unclassified-Unlimited Subject Category 39

19. Security Classif.(of this report)	20. Security Classif.(of this page)	21. No. of Pages	22. Price
Unclassified	Unclassified	89	A05

For sale by the National Technical Information Service, Springfield, Virginia 22161

NASA Langley Form 63 (June 1985)